

GEOLOGY OF THE GANOS FAULT ZONE IN THRACE

FIELD TRIP GUIDEBOOK

2006

**ARAL I OKAY*, CENK YALTIRAK* & LEONARDO
SEEBER****

*Istanbul Technical University, Eurasian Institute of Earth Sciences
and Department of Geology, Faculty of Mines
Ayazaga 80626 Istanbul, Turkey
okay@itu.edu.tr
yaltirak@itu.edu.tr

**Lamont-Doherty Earth Observatory, Palisades, NY 10964, USA, nano@ldeo.columbia.edu

CONTENTS

	Pages
PREFACE	1
INTRODUCTION	2
MORPHOLOGY OF THE GANOS FAULT ZONE	4
STRATIGRAPHY ALONG THE GANOS FAULT ZONE	7
Stratigraphy north of the Ganos Fault	7
Stratigraphy south of the Ganos Fault	7
Pleistocene marine terrace deposits	10
STRUCTURES ALONG THE GANOS FAULT ZONE	11
TEKİRDAĞ BASIN: AN ACTIVE HALF GRABEN	12
APATITE FISSION TRACK AND APATITE U/He DATA: IMPLICATIONS FOR THE EVOLUTION OF THE GANOS FAULT	13
DESCRIPTION OF FIELD STOPS	
İSTANBUL TO TEKİRDAĞ	16
Stop 1 - Folding in shales of the Mezardere Formation	18
Stop 2 - Steeply dipping tTurbidites of the Keşan Formation	21
Stop 3 - Recumbent kink folds in the Keşan turbidites	22
Stop 4 - Ganos Fault and the distal turbidites of the Gaziköy Formation	25
Stop 5 - The Gaziköy marine terrace deposits	28
Stop 6 - View of the Ganos Fault from the north	30
Stop 7 - 9th August 1912 Ganos earthquake surface break	30
Stop 8 - Panoramic view of the Ganos Fault from the Doluca Hill	31
Stop 9 - Eocene turbidites and debris flows south of the Ganos Fault	33
Stop 10 - Angular unconformity between the Eocene and Miocene sequences	33
Stop 11 - Blueschists and serpentinite in the Ganos Fault Zone	34
REFERENCES	36

PREFACE

This guidebook is prepared for the participants of the one-day excursion following the International workshop on Comparative Studies of the North Anatolian Fault and the San Andreas Fault (Southern California) to be held in the Istanbul Technical University between 14th and 16th August 2006.

The aim of the excursion is to introduce the structural, morphological and sedimentological features associated with the Ganos Fault Zone, the active segment of the North Anatolian Fault (NAF) in Thrace. The excursion is designed from a geologist point of view of a fault with interest in its evolution on a million year time scale. Specifically the question explored is how far is it possible to infer the evolution of a major fault from deformation in the fault zone. How much is the strain partitioned in a major fault zone?. Is the deformation - on a million year scale - concentrated on a limited width (a few hundred meters) or is it distributed over a wider fault zone? The Ganos Fault is a suitable place to explore such questions, as it cuts through a well exposed Tertiary sequence, known to be not significantly deformed outside the fault zone. By studying the deformation in the fault zone, it was thought possible to gain information on the progressive and finite deformation associated with the transpressive activity of the North Anatolian Fault, which is widely believed to have arrived in the Marmara region in the Pliocene. However, issues became more complicated when recent apatite fission track and apatite U/He dating showed that the Ganos Fault was active during the Late Oligocene and Mid-Miocene. Apparently the North Anatolian Fault used a pre-existing structure, and this makes differentiation of structures associated between the post-NAF Ganos Fault and a pre-NAF Ganos Fault a difficult task.

The guidebook is divided into two parts. The first part gives general background information on the Ganos Fault Zone, largely based on Okay et al. (1999, 2004), Seeber et al. (2004), Yaltrak et al. (2002) and Zattin et al. (2005). The second part of the guidebook describes the field stops. Detailed description of the field stops are provided, so that the guidebook can be used independently without further guidance. We will probably have not time to visit the few optional stops described at the end of the guidebook. Some of these stops, such as Stop 10 with the angular unconformity between the Eocene and Miocene sequences, illustrate critical geological features which have direct bearing on the recent discussions on the timing and arrival of the NAF in Thrace.

INTRODUCTION

The North Anatolian Fault is a major dextral transform fault, which accommodates the westward motion of the Anatolian Plate (Fig. 1). It extends for 1600 km from the Karliova triple junction in the east to the North Aegean Trough in the Aegean Sea in the west (Şengör, 1979; Barka, 1992; Hubert-Ferrari et al., 2002; Şengör et al., 2005). The North Anatolian Fault is thought to have nucleated in the eastern Anatolia in the Late Miocene and propagated westward reaching the Aegean region during the Pliocene-Quaternary. Along its entire length the North Anatolian Fault zone is associated with uplifts and depressions related to the segmentation and bending of the fault. The most prominent active depressions are the three basins, over 1000 m deep, in the Sea of Marmara (Fig. 2, Okay et al., 2000; Le Pichon et al., 2001; Armijo et al., 2002).

The Tekirdağ Basin in the western Marmara Sea and the adjoining Ganos Mountain, the main object of this field excursion, are forming around the Ganos fault bend between the Central Marmara and Ganos fault segments of the North Anatolian Fault (Fig. 2, Okay et al., 2004; Seeber et al., 2004). The Ganos bend is thought to mark the eastern termination of the 9th August 1912 M_S 7.4 earthquake rupture (Ambraseys and Finkel, 1987).

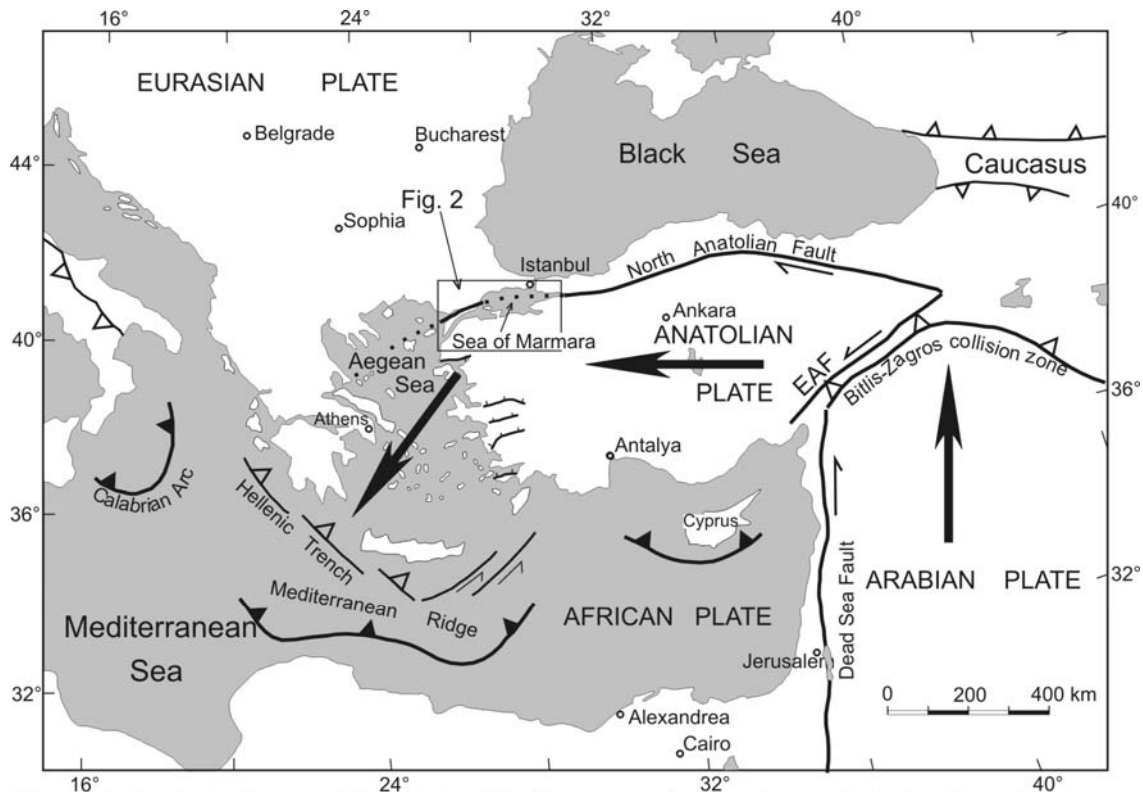


Fig. 1. Active tectonic map of the Eastern Mediterranean showing the geological setting of the Marmara Sea. Lines with filled triangles show active subduction zones, lines with open triangles are active thrust faults at continental collision zones, and lines with tick marks are normal faults. The large solid arrows indicate the sense of motion of the lithospheric plates. EAF, East Anatolian Fault.

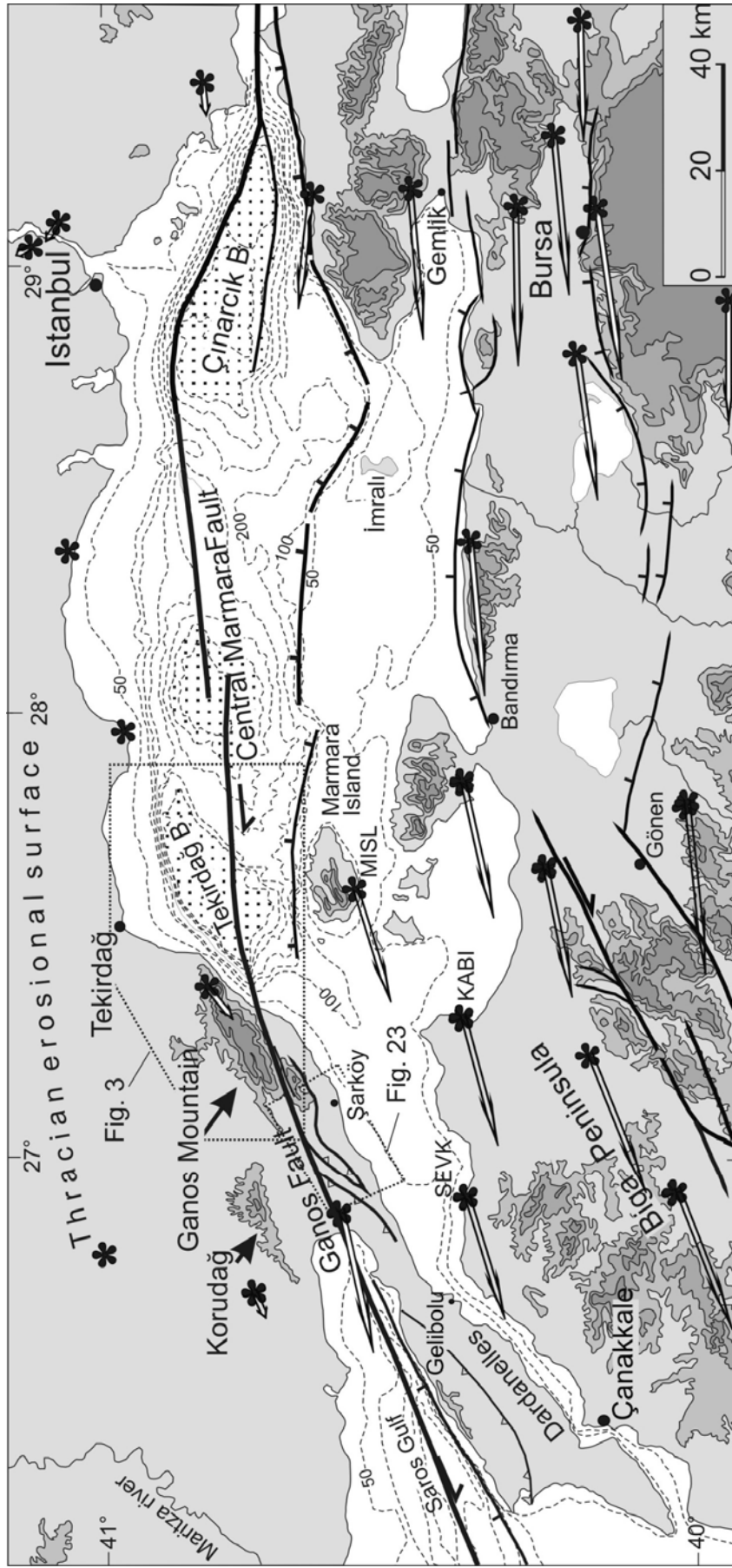


Fig. 2. Neotectonic map of the Marmara region, compiled from Şaroğlu et al. (1992), Okay et al. (1999; 2000), Le Pichon et al. (2001), Armijo et al. (2002). Faults shown cut Miocene or younger sediments. The bathymetric contours in the Marmara Sea are drawn at 50, 100, then at every 200 m. The topographic contours are at 300, 450 and 600 m. The stars and arrows indicate Global Positioning System (GPS) station localities and displacement vectors, respectively, with respect to the Eurasian plate (McClusky et al., 2000; Meade et al., 2002).

MORPHOLOGY OF THE GANOS FAULT ZONE

The Ganos Fault forms a prominent linear valley, 45-km-long between the Marmara and Aegean seas (Fig. 3). South of the Ganos Fault the morphology is characterized by broad ridges trending slightly oblique to the Fault. In contrast, the morphology north of the Ganos Fault shows a progressive change from a mountain in the east to a subsiding basin in the west (Fig. 2). The change in the morphology is at least partly related to an anticlockwise rotation of the displacement vectors towards the west. The Ganos Mountain, the principal interest during the field trip, is a region of anomalous uplift at the eastern end of the Ganos Fault (Figs. 2 and 3). It trends N70°E parallel to the Ganos Fault for ~35 km with a relatively uniform width of 8 to 11 km. The steep northern submarine slope of the Tekirdağ basin forms an integral part of the Ganos Mountain. The maximum relief of the Ganos Mountain is ~2000 m from the base of the Tekirdağ depression at -1120 m to the top of the mountain at 924 m. Towards the southwest the Ganos Mountain pinches out, and gives way to the Saros depression of the Aegean Sea, whereas towards the northeast it projects into the steep northern submarine slope of the Tekirdağ Basin (Figs. 2 and 3). The southern margin of the Ganos Mountain is defined by the Ganos Fault, and is characterized by very steep slopes reaching up to 50°. In the north, the Ganos Mountain is bordered by the Thracian plain, a large, flat-lying erosional surface at ~120 m formed probably during the Late Pliocene-Early Quaternary (Fig. 2, Okay and Okay, 2002). The abrupt transition from the Thracian plain to the Ganos Mountain is well marked on the morphology, and trends subparallel to the trace of the Ganos Fault (Fig. 3). This transition coincides with a monoclinial flexure suggesting that the morphology is also folded. The parallel alignment of the northern and southern margins of the mountain with the Ganos Fault indicates that the Ganos uplift is controlled by the Ganos Fault, as has been deduced in early studies (e.g., Şengör, 1979).

The Ganos Mountain forms essentially a single range made up of similar lithology, is relatively small, and has a uniform orientation. These geomorphic features coupled with the high rate of deformation in the region amounting to 20 mm/y, indicate that the morphology of the mountain can be used to chart the evolution of the recent vertical tectonics. Furthermore, because the mountain lies at the coast, changes in uplift and subsidence can be quantified using the sea level as a reference horizon. Fig. 4 shows cross-sections of the Ganos Mountain taken parallel and at right angles to the Fault. The cross-section parallel to the Ganos Fault shows an initial increase in uplift towards the east, which reaches a maximum at a location 2 km west of the coastline, and then fast subsidence farther east. This is also seen in the two cross-sections taken at right angles to the Ganos Fault, 11 kilometers apart (Fig. 4a). Between these two cross-sections the Ganos Mountain maintains or even accentuates its *relief* towards the east but have *subsided* by 1100 meters, with the northern submarine slope of the Tekirdağ Basin forming the direct submarine continuation of the southern flank of the Ganos Mountain. The eastward subsidence of the Ganos Mountain is also apparent in the geology, where the formation boundaries and average bedding strike out into the Marmara Sea (cf. Fig. 6).

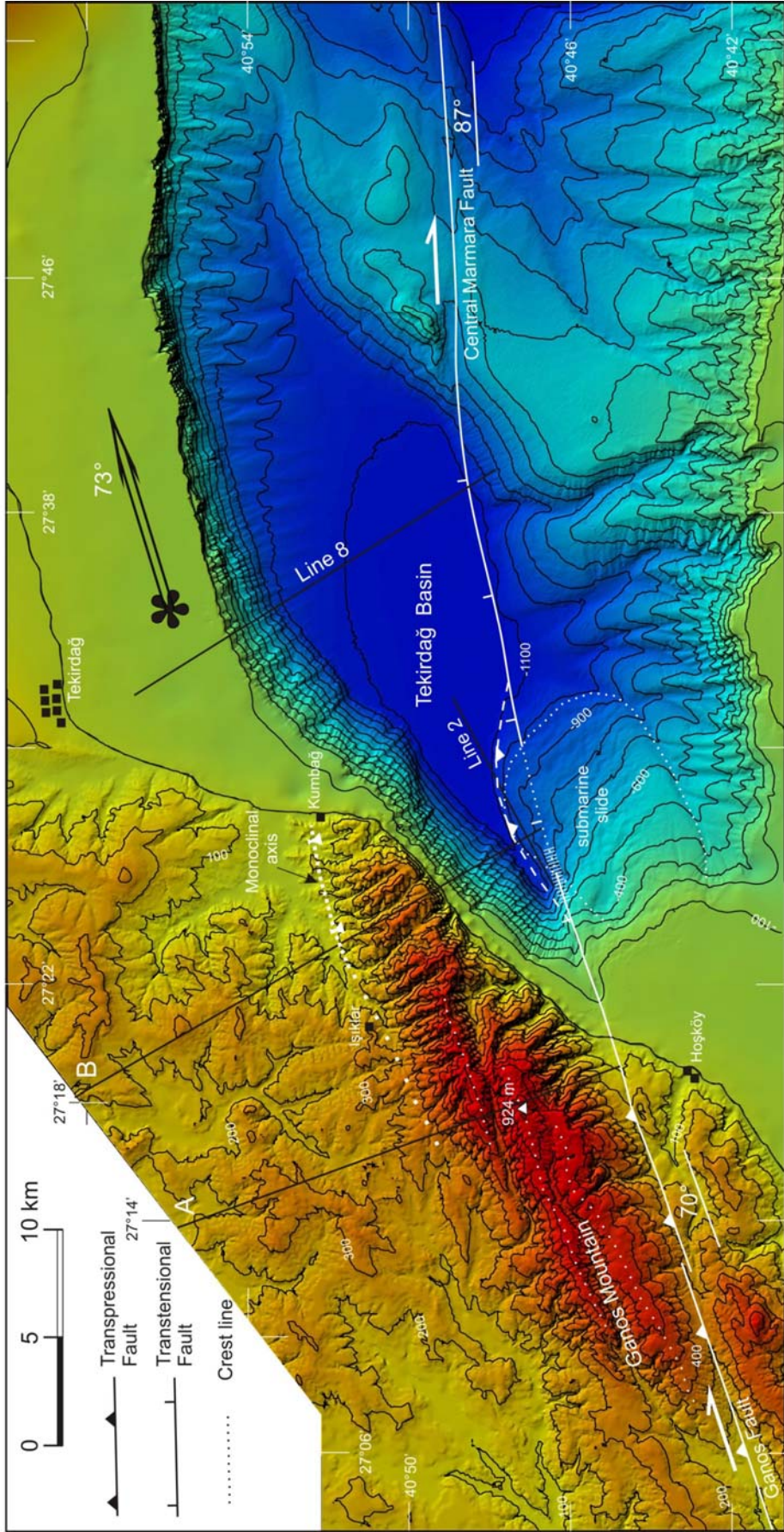


Fig. 3. Digital elevation model of the Ganos Mountain and the adjoining Tekirdağ Basin (from Okay et al., 2004). The topographic data were generated by digitising contour lines at every 20 m from 25 000 scale topographic maps. Shelf bathymetry is digitised from the bathymetric charts of SHOD (1983, 1988), whereas the bathymetry deeper than 100 m is from Rangin et al. (2001). The hatched segment on the North Anatolian Fault marks the transition from transpression in the west to transtension in the east with a N73°E displacement vector. The fault segment indicated by dashed lines north of the submarine slide shows the trace of the North Anatolian Fault in Le Pichon et al. (2001), Armijo et al. (2002), Demirbağ et al. (2003).

The subsidence of the Ganos Mountain is not uniform but increases towards the Ganos Fault indicating that the subsidence is largely achieved by southward tilting of the mountain. This can be deduced by comparing two subparallel cut-off lines in the cross-sections in Fig. 4a. The intersection between the topography and the Ganos Fault is off-set by 1100 m between profiles A and B, whereas that of the topography and the upper stratigraphic boundary of the Gaziköy Formation by only 500 m. Furthermore, *en bloc* subsidence would have created a basin north of the Ganos Mountain, which is not observed. Therefore most of the subsidence occurs by tilting with the tilt axis situated at about 10 km north of the Ganos Fault (Fig. 4a). Simple calculations indicate a southward tilting of $\sim 7^\circ$ between profiles A and B. Distributed normal faulting at high angles to the Ganos Fault with the fault plane consistently dipping to the northeast (see later) also contributes to the subsidence of the Ganos Mountain.

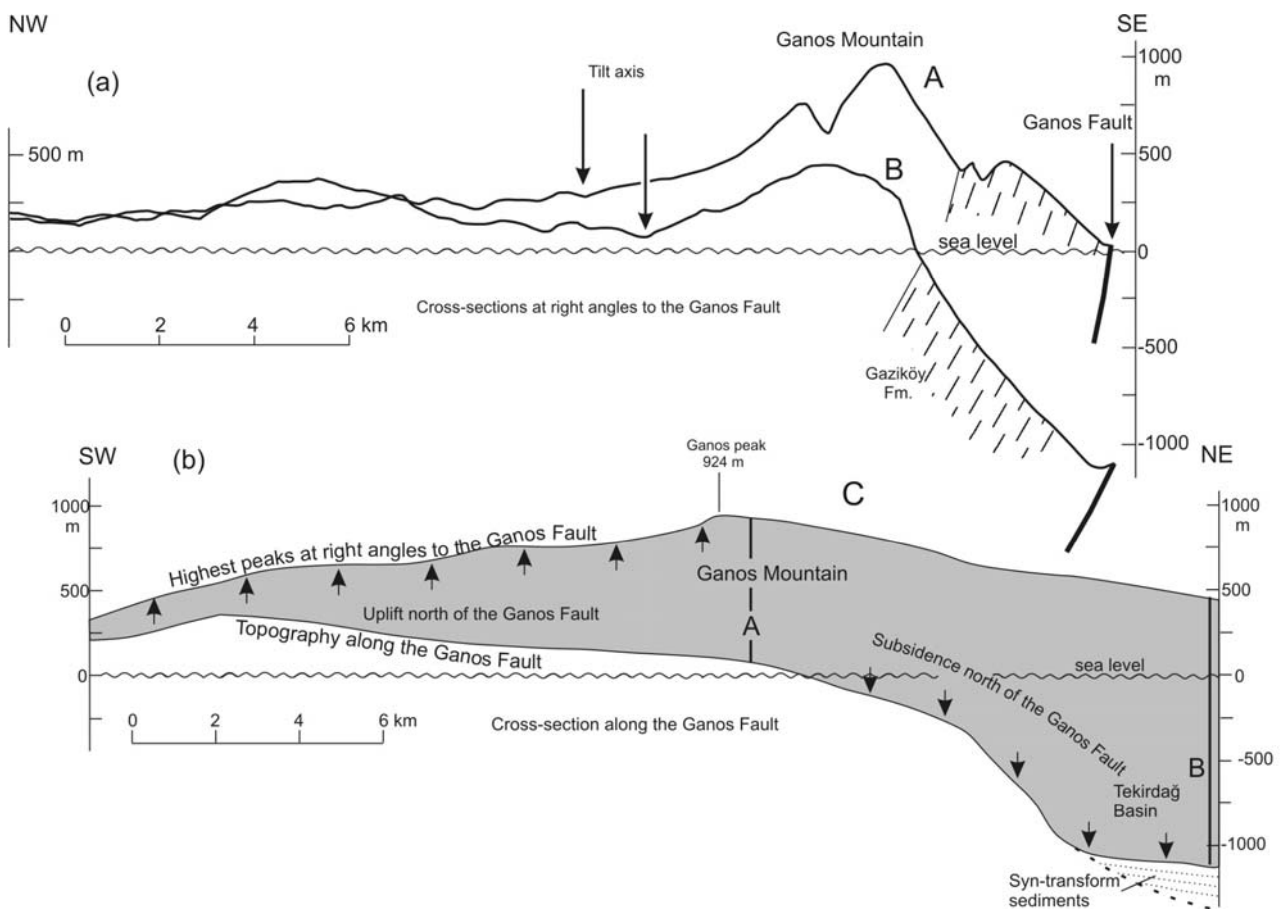


Fig. 4. (a) Cross-sections at right angles to the Ganos Fault (A and B). Note that although the profiles in A and B are similar, the profile at B has subsided by more than 1000 metres with respect to A. (b) Projection of the Ganos Mountain on a vertical Ganos fault plane. The lower line in the section shows the topography parallel to the Ganos Fault, and the upper line the highest peaks in the Ganos Mountain at right angles to it. For location of cross-sections see Fig. 3. Vertical exaggeration is four times.

Recently, microbathymetry and shallow stratigraphy were obtained from the region where the Ganos fault juts out to the Marmara Sea (Polonia et al., 2002; Seeber et al., 2004). Based on these data Seeber et al. (2004) also argue for subsidence and southward tilting of the north side of the Ganos Fault, the subsidence rate is estimated as 4-6 mm/y. With this rather high rate, the

subsidence between the profiles A and B in Fig. 4 can be achieved in 183 000 - 275 000 years, whereas the 11 km of strike slip displacement would take 550 000 years with a rate of 20 mm/y. These calculations indicate that the subsidence of the Ganos Mountain has been continuing since at least several hundred thousand years.

The subsidence by southward tilting also explains an apparent anomaly. Although the mountain is subsiding in the east, it is still characterized by very steep slopes overlooking the Marmara Sea. This produces a shoulder-type margin, where the drainage-divide lies close to the top of the escarpment (Fig. 3). These types of margins are usually explained by uplift at the foot of the escarpment. However, in this case rotational normal faulting leads not only to subsidence but also to an increase in slope angles by the southward tilting of the mountain face (Fig. 4a).

STRATIGRAPHY ALONG THE GANOS FAULT ZONE

The Ganos Fault cuts through the hydro-carbon-bearing Mid-Eocene to Oligocene Thrace Basin. The Thrace Basin consists mainly of siliciclastic turbidites, over 9 km thick in its central part (Kopp et al., 1969; Turgut et al., 1991; Görür and Okay, 1996). It is weakly deformed except along the Ganos and the now inactive Miocene Terzili faults. As there are some notably stratigraphic differences between the northern and southern sides of the Ganos Fault, they will be described separately below.

Stratigraphy of the northern block

North of the Ganos Fault the stratigraphy is best seen in the Ganos Mountain, which exposes Eocene-Oligocene siliciclastic rocks of the Thrace Basin, divided into four formations (Figs. 5 and 6). The Gaziköy Formation at the base consists dominantly of Eocene shale and siltstone with rare sandstone and andesitic tuff and basaltic lava interbeds and represents distal turbidites. The base of the Gaziköy Formation is not exposed; it has a minimum measured thickness of 855 m, and gradually passes up to the sandstone-shale intercalation of the Keşan Formation. The Keşan Formation has a thickness of over 3 km in the Ganos Mountain and consists of Upper Eocene proximal turbidites. It is overlain conformably by shales of the Mezardere formation, 750 m thick, representing prodelta mudstones. The shales of the Mezardere Formation are overlain by the thickly bedded Oligocene sandstones of the Osmancık Formation.

Stratigraphy of the southern block

An Upper Eocene-?Oligocene turbidite sequence, similar to the Keşan Formation but called Ceylan Formation forms the lowermost stratigraphic unit south of the Fault. The sequence is in part olistostromal and includes grain flows, debris flows with clasts of Upper Eocene limestone, serpentinite, blueschist, radiolarian chert, pelagic limestone and acidic magmatic rocks. Most of the blocks, which may reach one-km in size are derived from a Cretaceous oceanic accretionary prism. The Eocene-?Oligocene sequence is unconformably overlain by a sandy Miocene

sequence, more than one kilometer thick. The angular unconformity between the Eocene/Oligocene and Miocene rocks marks a significant phase of Late Oligocene uplift and deformation, confirmed by apatite fission track (AFT) dating (Zattin et al., 2004).

The Miocene sequence south of the Ganos Fault is divided into two formations. The Gazhanedere Formation at the base consists of variegated sandstone, mudstone and conglomerate and has a thickness of 500 to 700 m. The overlying Kirazlı Formation consists of pale yellow, grey, poorly cemented sandstones with a minimum thickness of 700 m. Based on microvertebrate fossils the Gazhanedere and Kirazlı Formations are assigned a late Early Miocene (Oerlanian approximately equal to Burdigalian-Early Langhian) and Middle Miocene (Astracian corresponding to Langhian-Serravalian) ages (Ünay and de Bruijn, 1984).

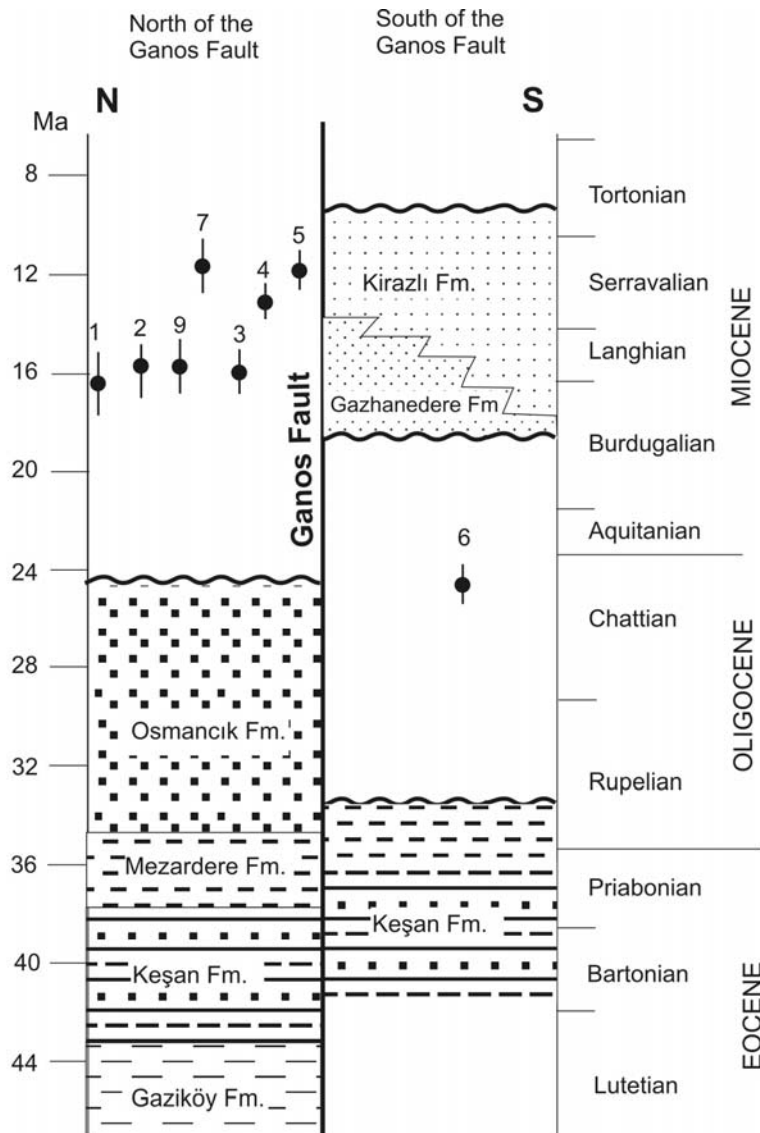


Fig. 5. The stratigraphy north and south of the Ganos Fault. The black circles indicate the apatite fission track ages from the Eocene Keşan Formation north and south of the Ganos Fault (Zattin et al., 2005).

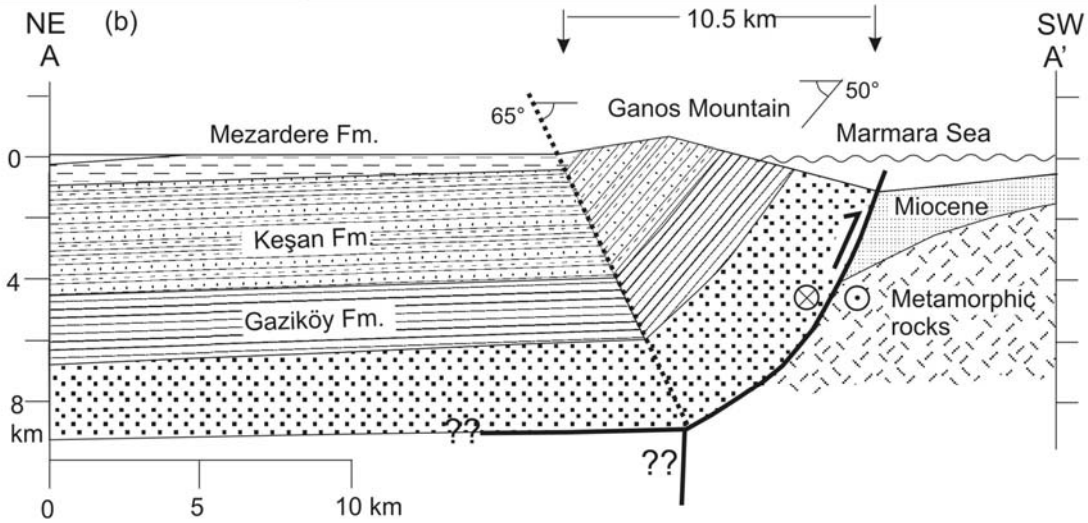
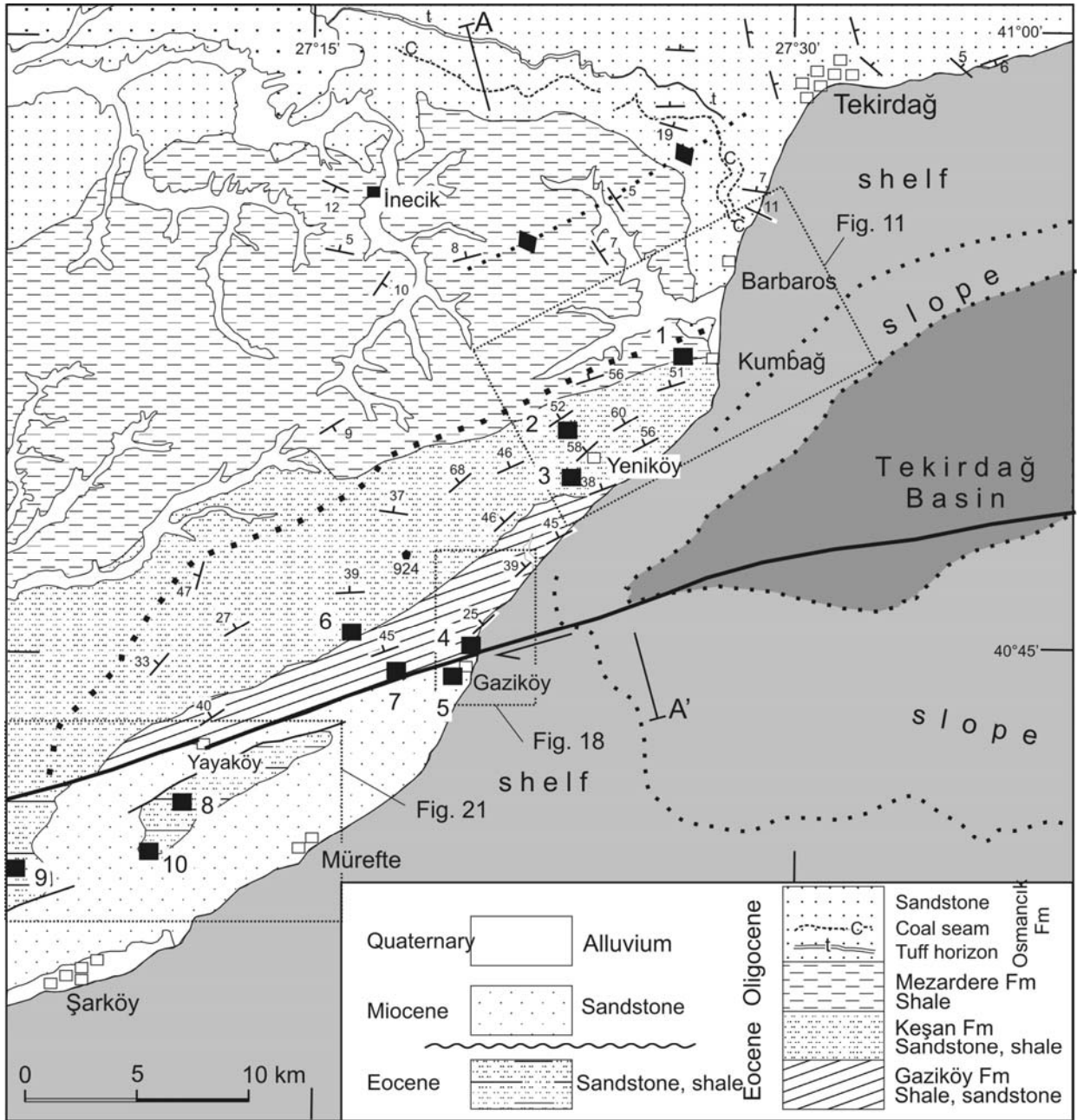


Fig. 6. Geological map and cross-section of the Ganos Mountain and the surrounding region showing the Stop localities. For location see Fig. 2. The dotted line shows the northern margin of the Ganos Mountain (after Okay et al., 2004).

Pleistocene marine terrace deposits - the Marmara Formation

Isolated but widespread Pleistocene marine terrace deposits, called the Marmara Formation, occur throughout the northern margin of the Sea of Marmara (Fig. 7, Sakıncı and Yalıtırak, 1997; Yalıtırak, 2002). The thickness of the Marmara Formation ranges from a few tens of centimeters up to 37 m. Their erosional base lies between 4 m and 40 m above the present sea level. Mediterranean type faunas, including *Ostrea* sp., occur widely in the Marmara Formation. The bivalve and gastropod faunas in the Marmara Formation are similar to the Upper Pleistocene (Tyrrhenian) faunas of the Mediterranean region. U/Th dating from in situ shells, reported by Yalıtırak et al. (2002), confirmed the Upper Pleistocene age, and showed that they were deposited during the highstands of oxygen isotopic stages 7 and 5, between ~210 000 and ~53 000 years. The elevations of the marine terrace deposits along with their ages indicate that the entire western Marmara shelf has been rising at an average rate of ~0.40 mm yr⁻¹ since ~225 000 years.

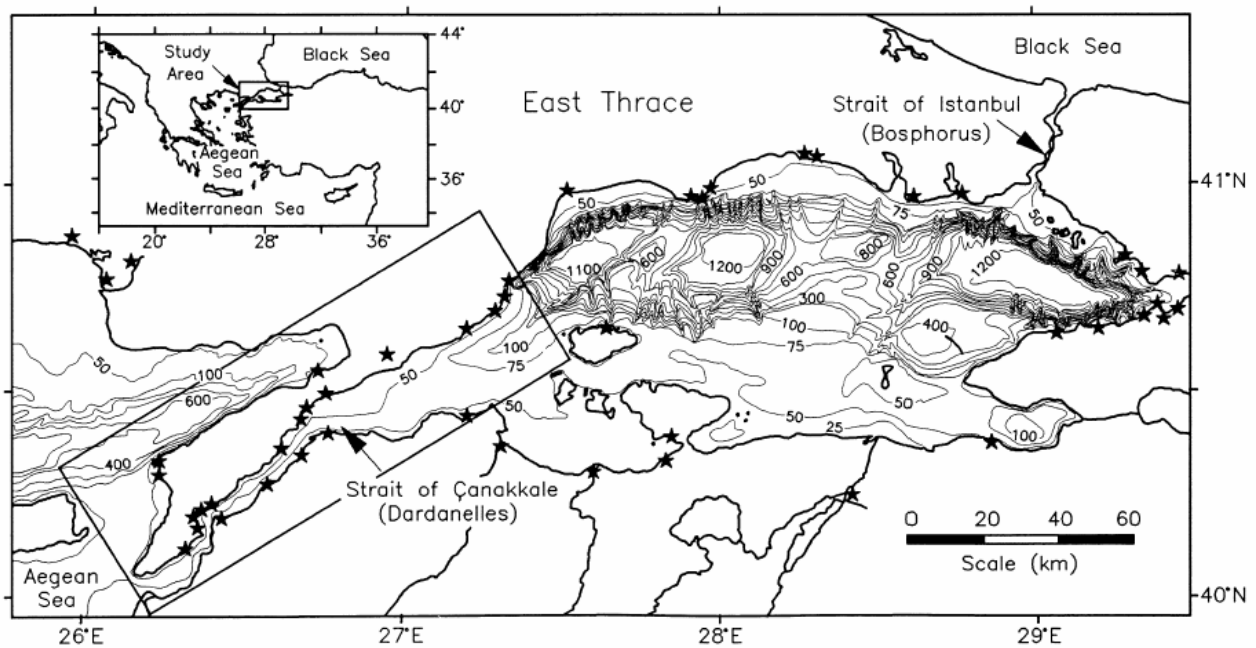


Fig. 7. Map of the Marmara Sea and environs showing the locations of Upper Pleistocene raised terraces (stars) (from Yalıtırak et al., 2002)

STRUCTURES ALONG THE GANOS FAULT ZONE

The structures observed south and north of the Ganos Fault are different. South of the Ganos Fault the Miocene sequence is deformed by minor thrusts trending oblique to the Ganos Fault, and by large number of small and gentle anticlines and synclines with the fold axis trending oblique to subparallel to the Ganos Fault (Fig. 2, Yaltrak, 1995; Tüysüz et al., 1998; Okay et al., 1999).

In contrast, the structure northeast of the Ganos Fault is characterized by a crustal scale monoclinial flexure. The Ganos Mountain forms the steep limb of this monocline and the low-lying hinterland in the north the flat limb (Fig. 6). The steep belt lies largely within the turbidites of the Gaziköy and Keşan formations, whereas the flat belt is in the shales and sandstones of the Mezardere and Osmancık formations. The hinge of the monocline trends parallel to the Ganos Fault and coincides closely with the northern margin of the Ganos Mountain (Fig. 3). The sedimentary structures in the sandstones in the steep limb of the monocline indicate that the beds dipping south are invariably inverted, and those dipping north are upright. This is achieved through recumbent kink-type folding with subhorizontal axial planes. The features and genesis of these enigmatic folds are discussed in the section on the description of field stops.

The oldest rocks are exposed adjacent to the Ganos Fault, and the sequence becomes younger towards north-northwest away from the fault (Fig. 6). The strike of bedding and that of the formation boundaries are subparallel to the Ganos Fault within a 10-km-wide zone north of the fault, however, farther north the structures are highly oblique (Fig. 6). This is the case for the boundary between the Osmancık and Mezardere formations west of Barbaros, and for the coal seams in the Osmancık Formation, which define a large and gently east-northeast plunging anticline (Fig. 6). This observation suggests a transition from structures apparently unaffected by the Ganos Fault to those controlled by the fault occurs at a distance of about 10 km north of the fault.

In the Ganos Mountain the common faults are NW-SE trending and northeast-dipping mesoscopic normal faults with an average fault plane orientation of 125/69 NE generally with throws from a few centimeters to several meters. They post-date the formation of the recumbent folds. The average normal fault (122/65NE) subtends an angle of 52° with the trace of the Ganos Fault. The normal faults may be related to the secondary extension in a dextral transpressive regime, and/or to the subsidence of the Ganos Mountain near the Ganos bend. Normal faults striking nearly at right angles to the Ganos Fault (N149°E) have been described in the Miocene sandstones south of the fault (Hancock and Erkal, 1990) and in the Gelibolu Peninsula (Tüysüz et al., 1998). Although the Ganos Fault is under transpression, reverse faults are rare in the Ganos Mountain, and the shortening is achieved largely by folding. Although shown in some speculative sections, no large scale thrusts are mapped in the Ganos Mountain.

South of the Ganos Fault there are several thrusts and folds slightly oblique to the trend of the Fault (Fig. 2). They affect the Miocene sequence and are related to the activity of the North Anatolian Fault.

TEKİRDAĞ BASIN: AN ACTIVE HALF-GRABEN

Ganos Mountain is bounded in the east by the Tekirdağ Basin, a rhomb-shaped depression with a side-length of ~15 km and an area of ~220 km² (Figs. 2 and 3). The Tekirdağ Basin has a flat-lying floor at ~1100 m depth bordered in the north and south by steep submarine margins. The Central Marmara Fault constitutes the southern margin of the Tekirdağ Basin, and the basin floor rises gently south of this fault towards the southern shelf at -100 m. In the north the Tekirdağ Basin is bounded by the steep northern submarine slope with slope angles of 11 to 23°.

The Tekirdağ Basin has been recently studied by multi-channel seismic reflection, high resolution bathymetric, sparker and deep-towed seismic reflection surveys (Okay et al., 1999; Le Pichon et al., 2001; Armijo et al., 2002; Parke et al., 2002; Seeber et al., 2004). These studies have shown that this basin is filled with Pliocene to Recent syntransform strata up to 2.5 km thick. A representative multi-channel seismic reflection section at a high angle to the Central Marmara Fault is shown in Fig. 8. The basin fill is strongly asymmetric, with the syn-tectonic growth strata thickening from essentially zero at the edge of the northern slope to 2.5 km at the Central Marmara Fault. In the top few kilometers, as observed in the seismic sections, the Central Marmara Fault dips north at ~60°, with the dip angles increasing eastward (Okay et al., 1999). As argued in Seeber et al. (2004), the strongly asymmetric basin fill, and the gradual downward increase in the dip of the syntransform beds, imply a shallower dip of the fault plane, and hence a listric fault profile. This is consistent with the data from Ganos Mountain, as discussed above.

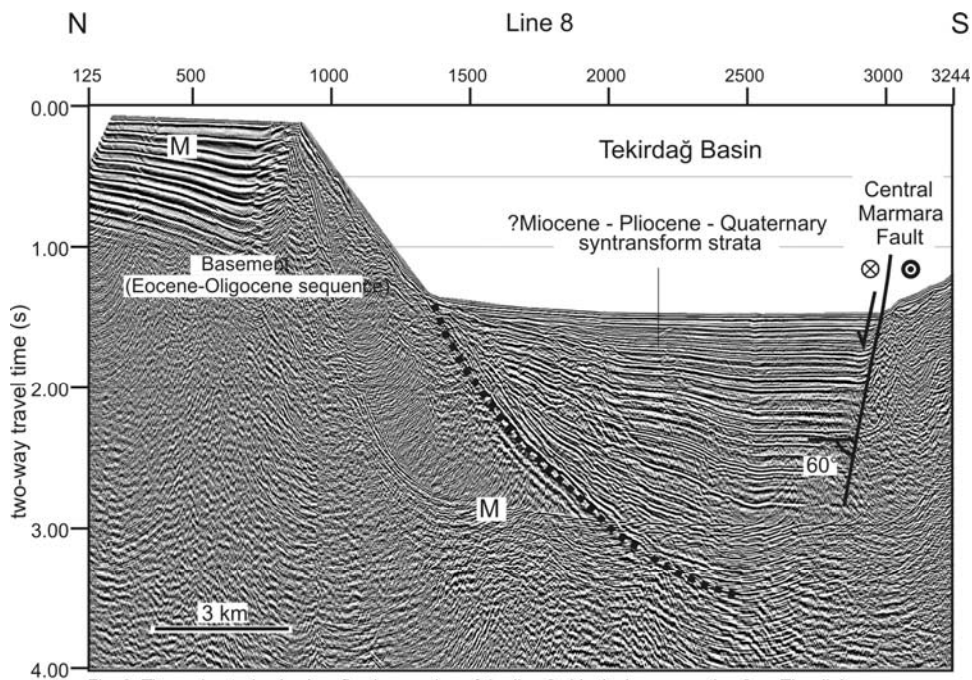


Fig. 8. Time-migrated seismic reflection section of the line 8. Vertical exaggeration 3 x. The digits are common depth point (CDP) numbers. Multiple reflections are indicated by M. The vertical exaggeration shown is an average and approximate value for the syn-transform sediments. See Fig. 3 for the profile location, and Okay et al. (1999) for details of seismic data collection and processing (after Okay et al., 2004).

APATITE FISSION TRACK AND APATITE U/He DATA: IMPLICATIONS FOR THE EVOLUTION OF THE GANOS FAULT

The Ganos monocline controls the present topography indicating that it is a relatively young structure. Therefore, apatite fission track (AFT) and apatite U/He techniques can be utilized to estimate the age of the Ganos monocline and indirectly the age of the Ganos Mountain. The AFT and the apatite U/He ages indicate the time when the rocks cooled below 110°C (about 4 km of overburden) and 70°C (2-3 km overburden), respectively. Sandstones from the Eocene Keşan and Gaziköy formations were used for AFT and apatite U/He dating. The AFT dates range from 16 Ma from the top of the Ganos Mountain to 12 Ma at the sea level very close to the Ganos Fault (Fig. 9; Zattin et al., 2005). The as yet unpublished apatite U/He ages range from 9,4 Ma from the top of the Ganos Mountain to 5,8 Ma at the sea level (Fig. 9). Furthermore, an Eocene sandstone taken from south of the Ganos Fault gave an AFT age of 24,7 Ma, whereas sandstones of similar Eocene depositional age taken from north of the Ganos Fault are characterized by Miocene ages of 16 Ma to 12 Ma. This indicates that there was relative vertical movements between north and south of the Ganos Fault during the Late Oligocene with the implication that the Ganos Fault essentially in its present location was in existence at the Late Oligocene (Zattin et al., 2005). The published data included only a single AFT age from south of the Ganos Fault (Fig. 9). However, since the publication of Zattin et al. (2005), other Eocene sandstone samples from south of the Ganos Fault gave similar latest Oligocene ages confirming the conclusions of Zattin et al. (2005). The AFT age and U/He apatite data were unexpected and surprising and have many important implications.

The crustal block south of the Ganos Fault was exhumed across the AFT closure isotherm (110 °C) in the latest Oligocene, while the northern block was exhumed later (16,4-11,7 Ma, mid-Miocene) (Fig. 5). Such different AFT ages for samples of similar age and lithology suggest that the Ganos Fault was active during the Late Oligocene.

The time-temperature modeling of the AFT data (Zattin et al., 2004) indicate a fast rate of cooling during the Mid-Miocene, at 10-11 Ma. This and the distribution of AFT ages indicate that the Ganos monocline was mostly formed by the Mid-Miocene, hence it is not a Plio-Quaternary structure.

Seismic reflection profiles in the Marmara Sea show that the NAF in the Tekirdağ basin dips listrically towards the northwest (Okay et al., 2004; Seeber et al., 2004) thus suggesting that the mid-Miocene uplift of the northern block might have occurred above a northwest dipping contractional or transpressional Ganos Fault (Fig. 10). This reconstruction is supported by the absence of Miocene sediments immediately north of the fault and by their presence immediately south of it.

Apatite U/He data show that the samples cooled below 60 °C by the Late Miocene or earlier. A sample collected at sea level close to the Ganos Fault gave an apatite U/He age of 5,8 Ma,

indicating that the maximum cumulative vertical displacement during the Pliocene and Quaternary has been less than two kilometers.

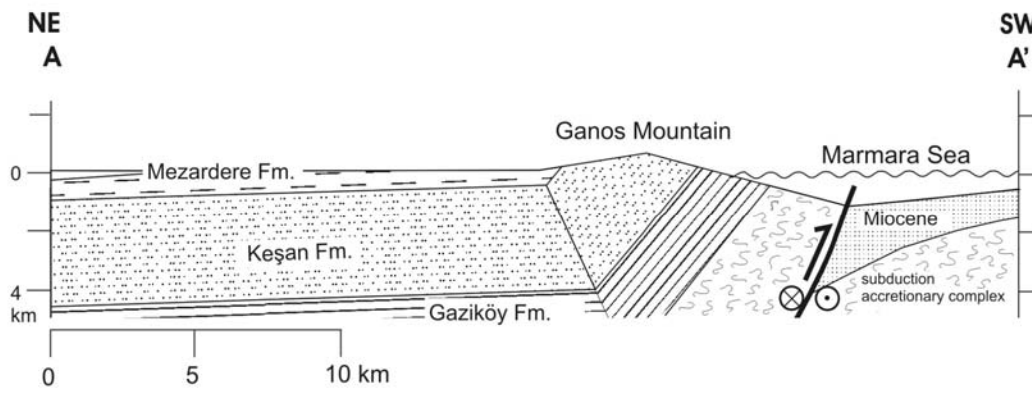
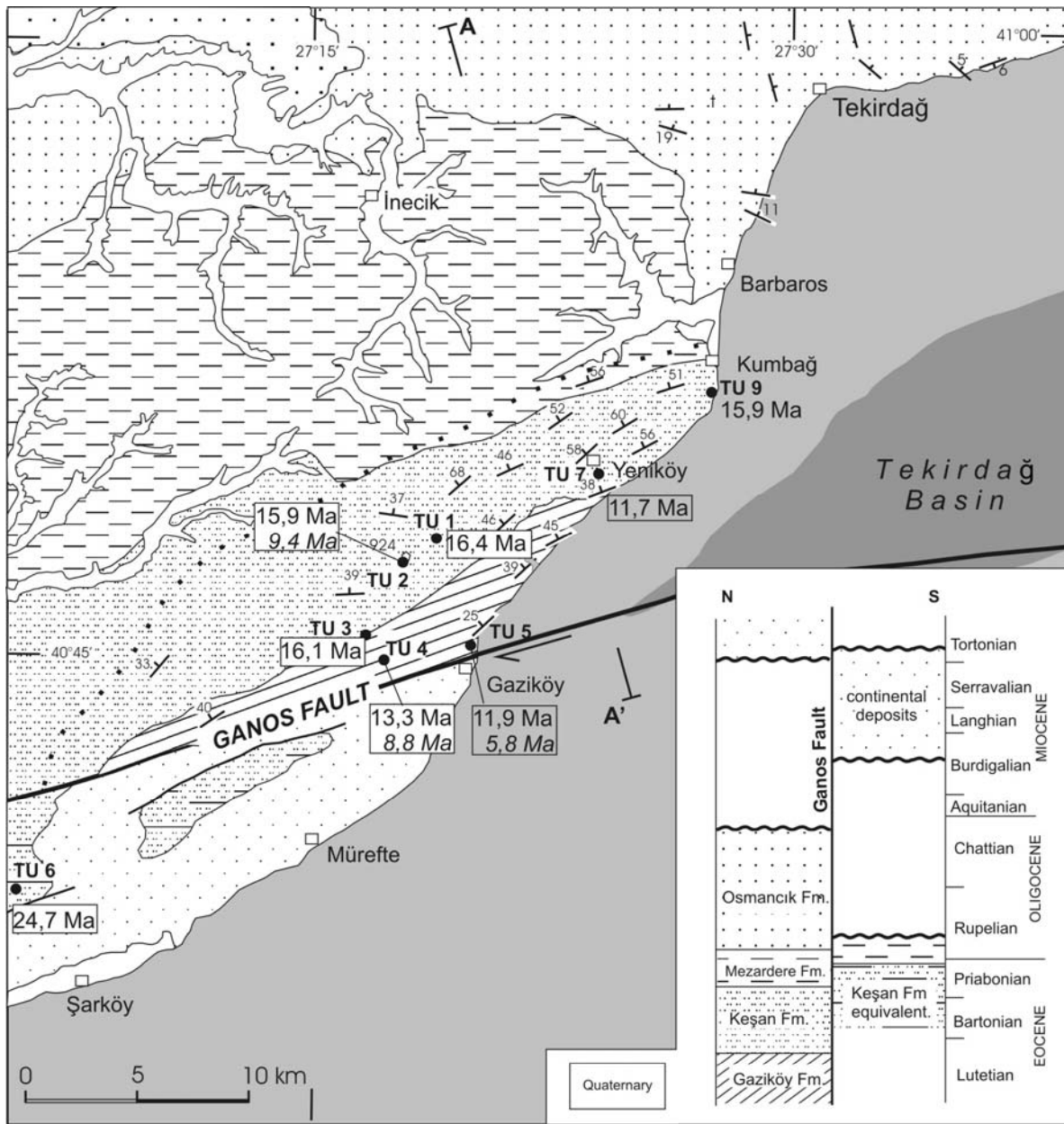


Fig. 9. Geological map and cross-section of the Ganos Mountain and the surrounding region with the localities of the geochronological samples and apatite fission track and apatite U/He (italics) ages. Exact duration of Oligo-Miocene hiatuses north and south of Ganos fault are poorly constrained (after Zattin et al., 2005).

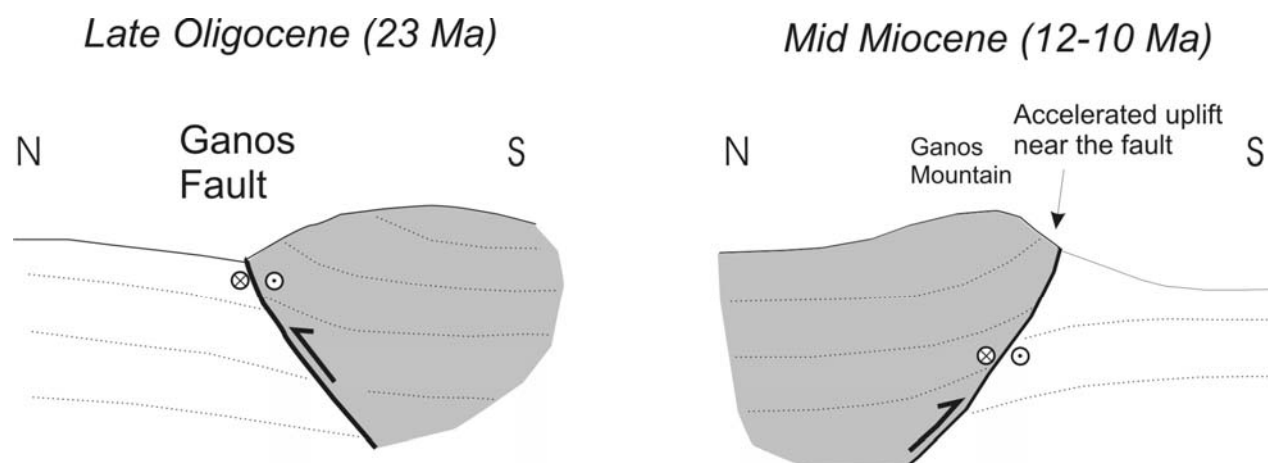


Fig.10. Schematic sketches illustrating possible behaviour of the Ganos Fault during the Late Oligocene and Mid-Miocene.

DESCRIPTION OF THE FIELD TRIP STOPS

İSTANBUL TO TEKİRDAĞ - ROAD LOG

We leave Istanbul early in the morning from the İTÜ campus, setting the meter to zero at its gates. The city of Istanbul, including the İTÜ campus site, is mostly built on Paleozoic (Ordovician to Carboniferous) sedimentary rocks. The campus is close to one of the junctions of the Edirne-Ankara motorway, which we will take to drive towards Edirne. The motorway follows the northern margin of the concrete jungle of suburban İstanbul. Carboniferous sandstones are exposed north of the motorway around the reservoir. The white rocks near the toll booths (at 21.9 km) are Miocene marls and clays, which crop out in southern part of European Istanbul. They tend to amplify the seismic acceleration; during the 17th August 1999 earthquake there was extensive damage in the southern part of European Istanbul, especially at Avcılar, built on Miocene clay and marl.

The motorway crosses the northern margin of the lagoonal lake of Küçükçekmece via the Yarımburgaz viaduct. A quarry wall of Eocene (Bartonian) reefal limestones can be seen north of the viaduct (at 26,5 km). A large cave in these Eocene limestones (Yarımburgaz) next to the Küçükçekmece Lake contains middle Pleistocene (390 000 - 161 000, Lower Paleolithic) human artifacts and constitutes the earliest evidence of human habitation in Istanbul. Farther on the satellite towns along the motorway (at 31-32 km) are built on Eocene limestone and marl.

At 43.8 km there is good view to the Çatalca ridge, a fault-bounded horst-like feature extending NW-SE on the western margin of the lake of Büyükçekmece. The motorway crosses the northern part of the lake through a long viaduct and climbs up the Çatalca ridge. The ridge is made up of metamorphic rocks unconformably overlain by Eocene limestones. The Eocene limestones are extensively quarried for gravel, and hence the large white patches on the landscape. The Çatalca ridge is located along a NW trending major pre- Late Miocene dextral strike-slip fault, which constitutes a major terrane boundary. The fault is not active, and the clustering of small earthquakes in the Çatalca region, seen in seismological maps, is due to the frequent and extensive quarry blasting.

After crossing the Çatalca ridge, marked by a large unfinished satellite town (Tepekent at 53.4 km), we are in the Thrace basin proper. The Thrace basin is filled by predominantly clastic sediments, up to 9-km-thick, of Middle Eocene to latest Oligocene age. The sequence shows a regressive development and ranges from Mid-Eocene distal turbidites to Upper Oligocene fluvial sandstones and lignite. The motorway crosses the poorly exposed Oligocene sandstones and shales of the Osmancık Formation. The large number of houses along the

Marmara coast are holiday homes for Istanbulers and extent almost without interruption from İstanbul to Tekirdağ and farther west. We pass the Kumburgaz (at 56.6 km), Selimiye (64.2 km) and Silivri (76.2 km) junctions and leave the motorway at Kınalı-Tekirdağ junction at 83 km. The landscape after the Silivri junction is typically Thracian - a bland landscape with long, broad valleys and hills covered by sunflower fields. The landscape is peppered with tumuli - small man made hills bearing the graves of the chieftains of the Thracian tribes. Two such tumuli can be seen on the horizon on the right after the toll booths at 86 km.

At 92.5 km we join the Istanbul-Tekirdağ highway (E-5). The highway is being widened to make it double lane, and this has opened several new roadcuts of buff, yellow, thickly bedded sandstones of the Oligocene Osmancık Formation (at. 94.7, 103.5, 104.0, 106.8 km's etc.). There are several gas fields in these sandstones; the sandstones are generally shallowly dipping except at major fault zones. The steep dips at 104 km are associated with the Miocene Terzili fault zone, a major NW trending dextral strike-slip fault.

At 106.8 km we pass through the liquid natural gas storage tanks of Botaş, and at 110.5 km from the outskirts of the town of Marmara Ereğlisi built on a promontory. The highway cuts through the innumerable holiday homes of Istanbulers. On a clear weather at 134.5 km next to the disused Salat sunflower oil factory and again at 146.5 km, there are good views of the Ganos Mountain in the horizon, a major uplift on the coast of the Marmara Sea. At 137.8 km the road crosses a Thracian tumulus. During the enlargement of the road the tumulus had to be excavated. It was untouched since the IVth century B.C., and the remains including a beautiful golden crown, is on exhibit in the museum at Tekirdağ.

At 144.8 km we stop at a large market (Maxi) to buy provisions for lunch. After this short stop we will continue driving towards Tekirdağ. On this short stretch there are good roadside exposures of the subhorizontal sandstones of the Osmancık Formation (148-149 km); there is even a thin coal seam at 148.2 km; several lignite mines are in operation in the Osmancık Formation. We will not stop at Tekirdağ but continue driving west towards Malkara. At 154.2 km we pass through the Muratlı-Kumbağ junction and start climbing a long hill slope, called Devebağırta; apparently the camels (deve) in the caravans used to cry out loud (bağırta) when climbing up this hill, hence the name. At the top of the hill at 158.3 km there are two large petroleum filling stations (Namık Kemal). The Ganos Mountain can be seen to the left (south) of us. At 160.0 km we make a dangerous turn round to the other lane, and take not the first (to the Yayabaşı village) but the second village road to the Yazır and Naip villages at 160.7 km (UTM 05 36 155 - 45 32 597; 40° 56.580' - 27° 25.770'). The road to Naip takes us towards the Ganos Mountain, which is directly in front of us. Just before the village of Yazır, at 163.0 km, shales of the Mezardere Formation can be seen on the left (east); at 166.9 km there is a good view of the bluish grey clay quarries of the Naip village, which we visit shortly. In the village of Naip at 168.4 km we come to a junction and take the road to the left (east) and drive towards Kumbağ. At 169.2 km we take a small rough road to the right, which will take us to our first field Stop.

Stop 1 - Gentle folding in the shales of the Mezardere Formation (Upper Eocene-Oligocene)

Location: Clay quarries of Naip, west of Kumbağ (G18-b2) (Fig. 11) (UTM 05 36 195 - 45 25 149; 40°52.554' - 27°25.774'). The quarries can be reached by taking the rough dirt road which branches off from the main road between Naip and Kumbağ at UTM 05 36.012 - 45 25 598; 40°52.797' - 27°25.644'. Once in the dirt road always follow the road on the right.

Interest: Gentle folding of shales in the flat limb of the Ganos monocline

Description: The Oligocene Mezardere Formation consists predominantly of shales, which are well exposed in the clay quarries of Naip. The shales are thought to have been deposited in the deeper parts of a major delta. The river was flowing from the south from the present Marmara Sea. Structurally we are here in the flat limb of the Ganos monocline but close to the sharp fold hinge (Fig. 11). The shales are subhorizontal to gently folded. Here we see a large, upright gentle anticline with an ENE trending fold axis and with a half wavelength in excess of 500 m. Such folding is typical for the flat limb of the Ganos monocline.. The fold axis generally trend 80° with a wide scatter, (Fig. 12). The folding is probably Late Oligocene and indicate gentle shortening perpendicular to the trend of the Ganos Fault.

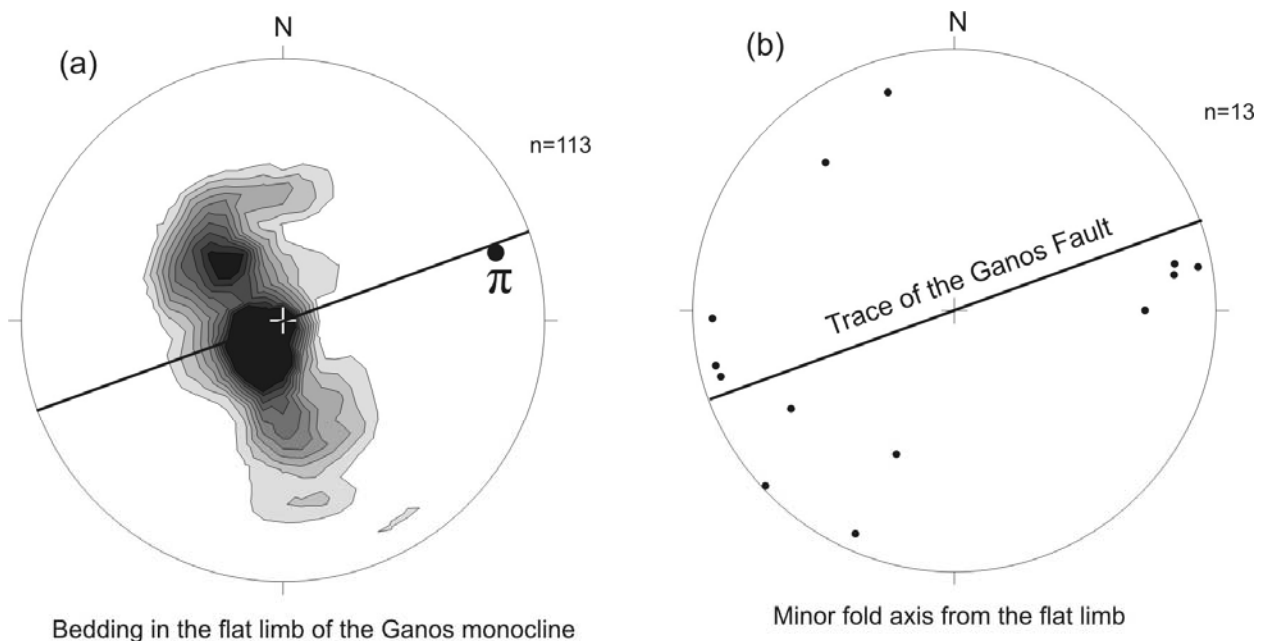


Fig. 12. Structural data from the flat limb of the Ganos monocline, northeastern Ganos Mountain. Equal area projections, lower hemisphere. Thick lines show the strike of the Ganos Fault (N70°E). (a) Contour plots of poles to bedding. The contours are at one percent intervals. (c) Fold axis of the upright folds.

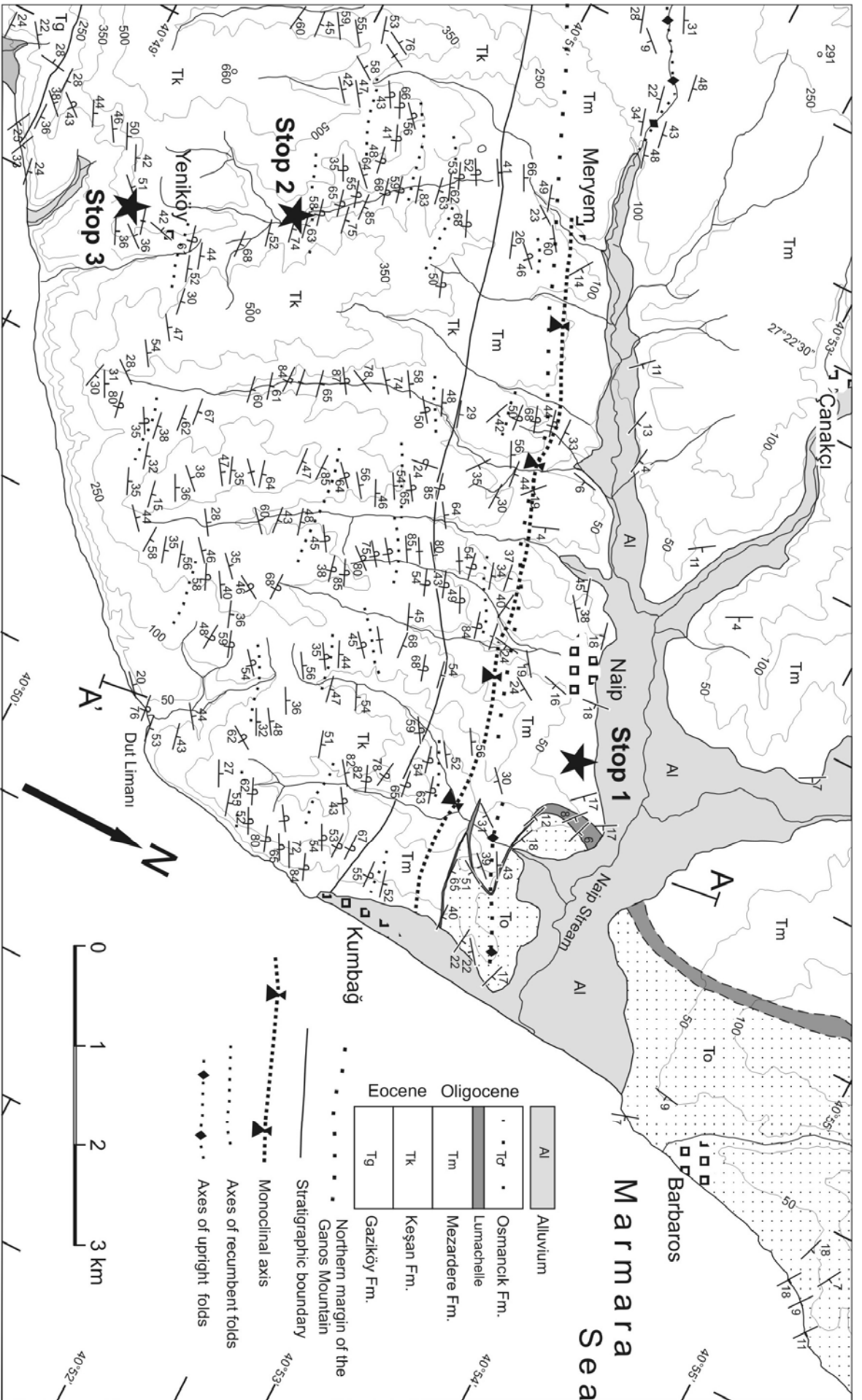


Fig. 11. Geological map of the Kumbağ region, eastern Ganos Mountain, showing the Stop localities. For location see Fig. 6 (Okay et al., 2004).

Refolding of earlier folds

In the Barbaros -Yeniköy region the bedding is subhorizontal in the flat limb of the monocline north of the Naip Stream (Fig. 11). The bedding in this region strikes generally northwest at high angles to the Ganos Mountain front and the Ganos Fault. However, as the monoclinical axis is approached the bedding is rotated to northeast strikes and is deformed into upright gentle folds with subvertical axial planes and northeast trending fold axes. This is well shown through the lumachelle horizon, which marks the base of the Osmançık Formation (Fig. 11). North of the Naip stream the lumachelle horizon strikes north-south, and forms part of the southeast limb of the large anticline described above (cf. Fig. 6). Traced south of the Naip Stream the lumachelle bed is refolded into upright folds, which become increasingly tighter towards the monoclinical axis (Fig. 11). This refolding of older folds is ascribed to the effect of the Ganos Fault. The bedding in the flat belt of the monocline forms a girdle around a fold axis 72/12NE, parallel to the trace of the Ganos Fault (Fig. 12). The minor fold axes in the flat belt trend generally northeast but are more dispersed compared with those from the steep belt, possibly as a result of interference of earlier folds (Fig. 12).

The transition from the flat to the steep limb of the monocline is abrupt, and closely coincides with the change in the slope angles indicating that the topography is also being deformed (Fig. 3). In several studies a fault has been placed north of the Ganos Mountain to explain the abrupt changes in the topography and structural style (e.g., Şaroğlu et al., 1992; Şentürk et al., 1998; Yaltrak and Alpar, 2002). Detailed sections in several well-exposed streams crossing the "fault" did not reveal any such tectonic boundary in the region studied. Furthermore, there is no significant stratigraphic omission or repetition along the boundary between the flat and steep belts, which would have been the hallmark of a major normal or reverse fault.

After the clay quarry we will drive back to the village of Naip, taking the same road as we used before. The meter is set zero at the Yazır-Naip junction. After the village of Naip we come to a road junction at 0.9 km, and take the road on the left, and drive parallel to the northern flank of the Ganos Mountain (Fig. 11). Shallowly dipping sandstones and shales of the Mezardere Formation can be seen on some road cuts. At 4.5 km we come across another road junction and take the road to the left (south) towards Şarköy. The road follows a valley, which cuts across the Ganos Mountain (Fig. 11). At 5.0 km we pass the village of Meryem (Mermer) and are now in the steep limb of the Ganos monocline within the subvertical sandstones and shales of the Keşan Formation.

Stop 2 - Steeply dipping turbidites of the Keşan Formation (Eocene)

Location: Between the villages of Meryem and Yeniköy (G18-b3) (Fig. 11). There are several good sections along this road, e.g., between 6.8 and 7.2 km or 7.8 to 8.7 km.

Interest: Steeply dipping, locally overturned sandstones and siltstones in the steep limb of the Ganos monocline. River terrace deposits.

Description: A turbidite sequence of sandstones and shales is beautifully exposed along the road between Meryem and Yeniköy. The sandstones generally dip steeply to the north-northwest. Sole marks are widespread at the base of the sandstones and indicate that some of the sandstone beds are overturned. The sole marks (mainly flute casts and current bedding) indicate that the paleocurrents were coming from the west-southwest in a direction parallel to the trend of the mountain and that of the Ganos Fault (Fig. 13). Note also the river terrace deposits about six meters above the present stream, a sign of recent active uplift.

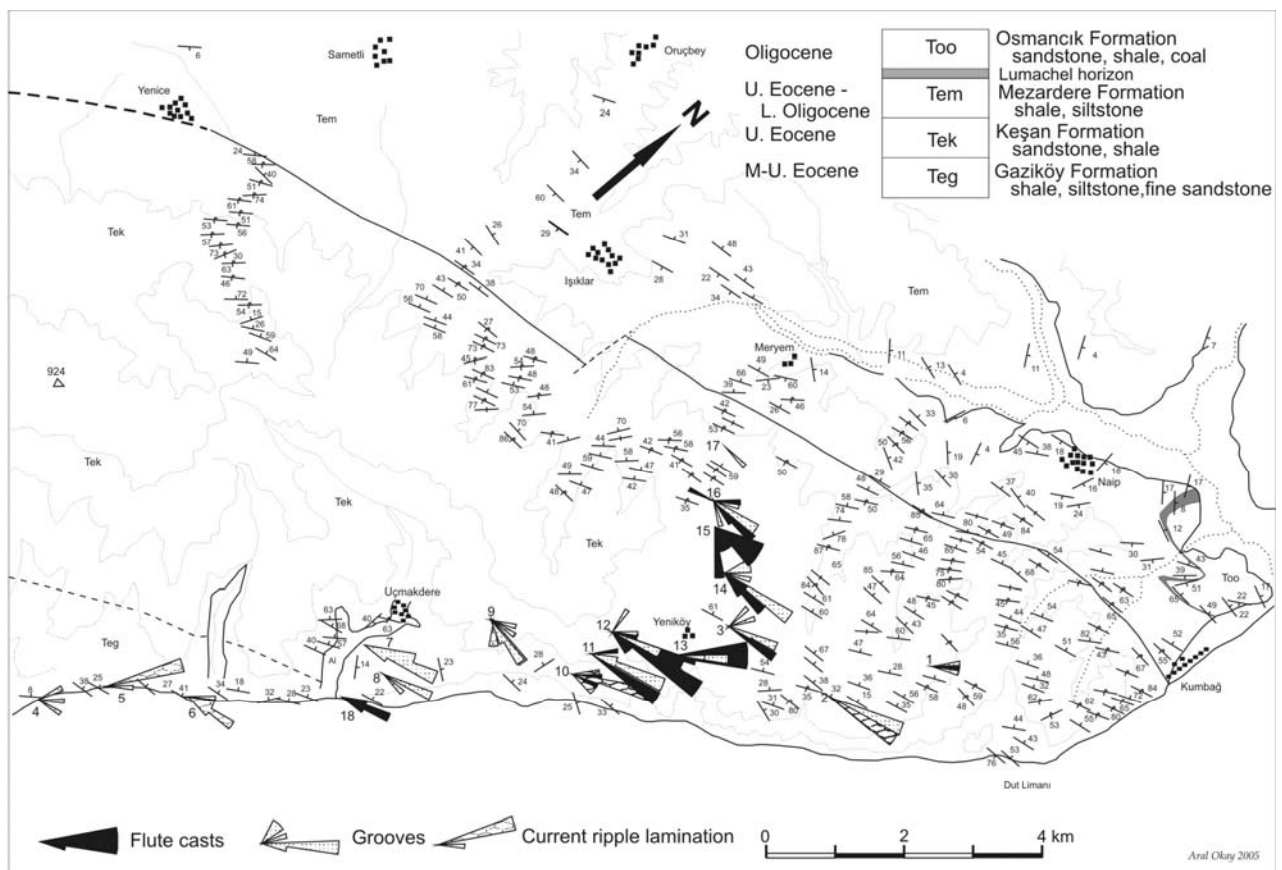


Fig. 13. Paleocurrents in the turbidites of the Gaziköy and Keşan formations (A. Okay and W. Cavazza, unpublished)

After walking a few hundred meters along the turbidites, we board the minibusses and drive towards Yeniköy, which we pass at 9.8 km.

Stop 3 - Homoclinal sequence in the steep limb of the Ganos monocline, recumbent kink folds, water shed close to the coast

Location: 600 m after the village of Yeniköy at 10.4 km (G18-b3) (Fig. 11) (UTM 05 33 888 - 45 19 157; 40°49.322' - 27°24.111')

Interest: Homoclinal sequence in the turbidites of the Keşan Formation (Eocene) in the steep limb of the Ganos monocline, recumbent kink folds, water shed close to the coast, large overturned kink fold in the steep limb of the Ganos monocline.

Description: A steeply northwest dipping sequence of sandstone and shale, defining the steep limb of the Ganos monocline, is beautifully exposed along the steep flanks of the Ganos Mountain overlooking the Marmara Sea. The Marmara island and the smaller uninhabited Hayırsız island can be seen directly in front of us. Both islands are made up of metamorphic and granitic rocks. A kink-type recumbent fold is exposed on the road cut; the south dipping beds are inverted.

Notice the deeply cut, steep-sided valley ending in the Marmara Sea. The local water shed lies very close to the coast passing through the village of Yeniköy. The stream we were following flows in the opposite direction. Another sign of coastal uplift.

We will walk along the road towards a large fountain at 11.0 km. A large recumbent kink-type fold is exposed behind this fountain (UTM 05 33 484 - 45 19 095; 40°49.289 - 27°23.823'). Because the fold axial plane is so sharp, it appears as a thrust. As usual the south dipping limb is inverted.

Recumbent kink-type folds in the Ganos region

The steep limb of the Ganos monocline is deformed by recumbent kink-type folds with subhorizontal axial surfaces (Fig.14), which results in the overturning of bedding. The overturning, which characterizes about a third of the bedding, is local on the range of a few



Fig. 14. Typical recumbent kink-type fold in the Eocene turbidites in Ganos Mountain. The folds are characterized by subhorizontal axial surfaces and hinge lines. The hinge lines are parallel to the trace of the Ganos Fault. In the folds the south dipping (to the left) limbs are invariably inverted. Note the boudinage in the fold hinge under the hammer.

meters to several hundred meters. The average bedding in the steep limb strikes northeast ($\sim 70^\circ$) parallel to the trend of the Ganos Fault and that of the mountain range (Fig. 15a). The normal and inverted beds form two distinct groups on the stereogram, centered on 64/42NW and 75/50SE respectively, giving an average regional fold axis of 69/04SW, parallel to the trace of the Ganos Fault.

Forty-four mesoscopic axes of recumbent folds show a variation in trend from N50°E to N96°E with a mean fold axis of 70/10NE, similar to the "average" fold axis of 69/04SW inferred from the bedding (Fig. 15b). The fold axial planes are dispersed around the horizontal with a dominance of southeast dips (Fig. 15c).

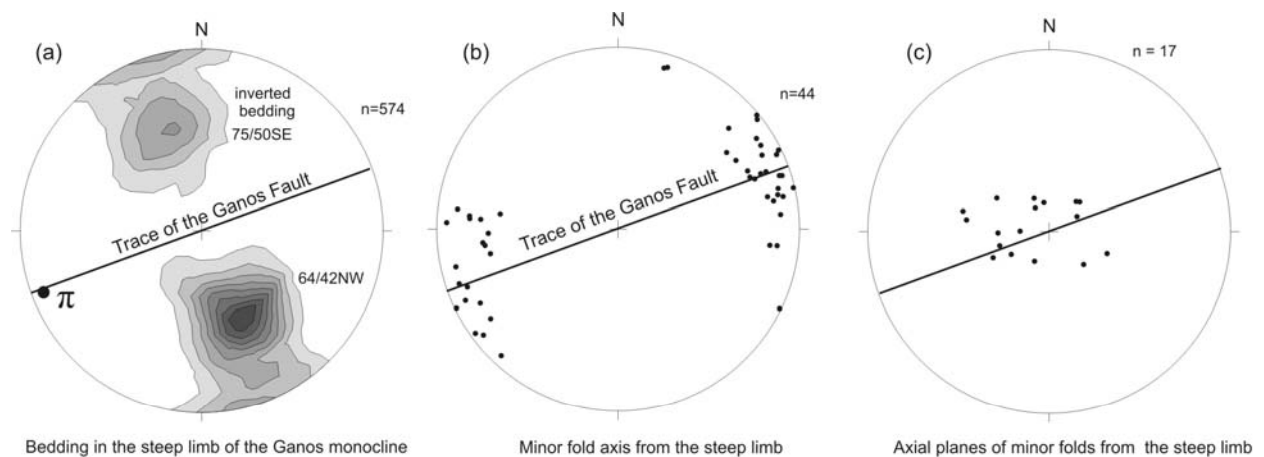


Fig. 15. Structural data from the steep limb of the Ganos monocline. Equal area projections, lower hemisphere. Thick lines in all projections shows the strike of the Ganos Fault plane (N70°E). (a) Contour plot of poles to bedding. The contours are at one percent intervals. (b) Minor fold axis of the recumbent folds. (c) Fold axial planes.

The folds have formed in the interbedded sandstone and shale beds and have wavelengths and amplitudes ranging from meters to hundreds of meters. They are generally parallel folds with straight limbs and sharp angular hinges with the interlimb angles of 65° to 120° . The strongly lithified sandstone beds maintain their thickness through the fold, whereas the shale interbeds locally show minor thickening in the fold hinges. Locally there are fractures in the outer arcs of the folded sandstone beds filled by shale (Fig. 14). These fractures are subparallel to the fold axis suggesting that they are produced through buckling rather than through extension parallel to the fold axis. Structures indicative of extension parallel to the fold axis, produced during rotation and characteristic for the strike-slip component of deformation (e.g., Harland, 1971; Jamison, 1991) were not observed. There is no cleavage associated with the folds. The folds are arranged en echelon, so that even the largest fold trace cannot be followed by more than a kilometer (Fig. 11). They usually die out laterally and vertically over short distances. The sandstone beds have been folded by flexural slip mechanism, whereas a combination of flexural slip and flow were effective in the folding of shale beds (e.g., Donath and Parker, 1964).

Absence of extension parallel to the fold axis indicates folding in a plane strain environment of northwest-southeast shortening under a single progressive deformation. Flexural-slip mechanism and the general absence of axial-plane cleavage indicate that the deformation occurred under low temperature and pressure conditions.

Folds formed in strike-slip shear zones share some common features, such as fold axes oblique to the shear direction, extension parallel to the fold axis, and upright fold geometry (e.g., Sylvester, 1988; Jamison, 1991). Minor folds in the Ganos Mountain do not show any of these features. The minor folds in the Ganos Mountain could have formed during NNW-directed simple shear of an inclined sandstone-shale sequence (Fig. 16). Some of the larger recumbent folds show stronger cataclasis in their inverted limbs, which supports the role of shear in the formation of these folds. The general southeast dips of the fold axial planes (Fig. 15c) are also in agreement with the model.

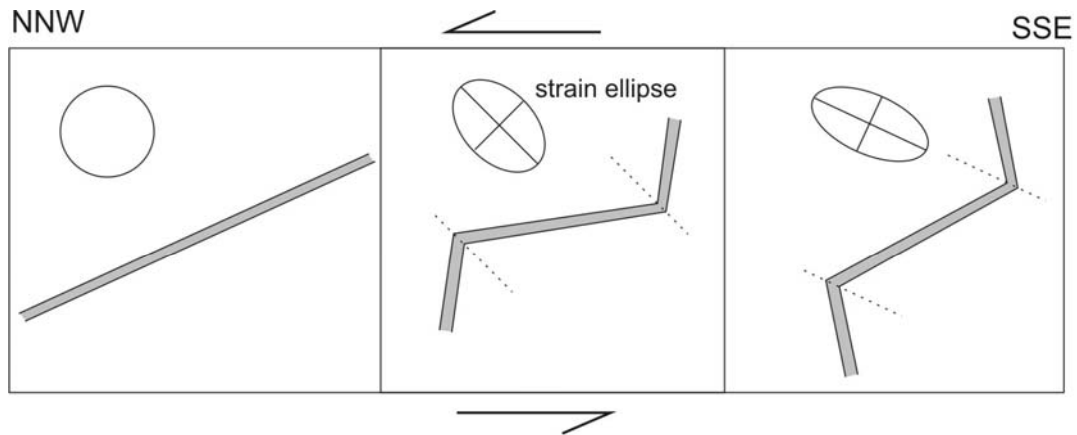


Fig. 16. Schematic model showing the formation of recumbent folds in the Ganos Mountain by rotation of the fold limbs. Time and deformation increases between panels from left to right.

An alternative mechanism for the origin of the recumbent kink-band folding is gravity-driven down-dip shortening of the Ganos monocline (Fig. 17).

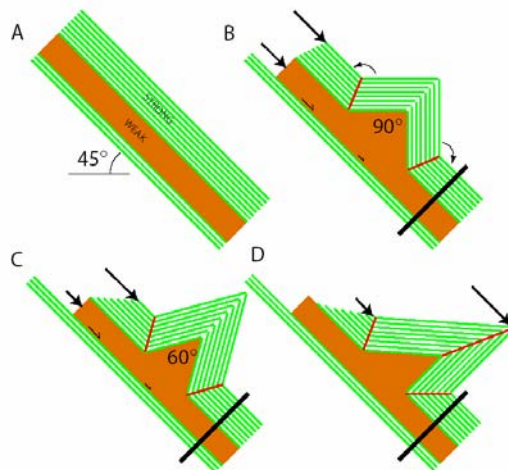


Fig. 17. Hypothetical kink-band folding by gravity-driven down-dip shortening of the Ganos monocline. Only configuration D would fit the observed distribution of bed attitudes.

ALTERNATIVE ROUTES

The planned excursion route includes driving from the village of Yeniköy to Gaziköy along the coastal road (route A). However, there is a distinct possibility that the road from Yeniköy to Gaziköy might be closed for road enlargement. In this case we will take an alternative route B.

Route A

From Stop 3 we continue by minibus and cross the well exposed turbidites of the Keşan Formation and pass through the quaint village of Uçmakdere, which earns a living from growing tobacco and grapes. After Uçmakdere the road follows the coast, and we are now in the Gaziköy Formation of dark shales and siltstones representing Middle to Upper Eocene distal turbidites. There are also a few thick acidic tuff horizons within the fine grained siliciclastics. The white color of some of the beds is due to coating by blocky vein calcite.

Stop 4 - Ganos fault and the structures in distal turbidites in its vicinity

Location: 600 meters north of the village of Gaziköy (G18-b4, c1) (Fig. 18, 19)

Interest: Ganos Fault as it enters the Sea, structures in the close vicinity of the Ganos Fault

Description: At this locality we are within 600 m north of Ganos Fault within the siltstones and shales of the Gaziköy Formation. What is perhaps surprising is that there is little in the structures to show that we are within close vicinity of one of the largest active strike-slip faults with a possible cumulative offset in excess of 60 km. The strain was strongly partitioned to a narrow brittle fault zone. The bedding in the siltstones and sandstones are well preserved. The only major structures are mesoscopic normal faults trending northwest and dipping 60°-80°, generally to the northeast with displacements ranging from a few centimeters to one meter (Fig. 17, 18).

A fine-grained sandstone sample from this locality gave a AFT age of 11.9 and an apatite U/He age of 5.8 Ma (Zattin et al., 2005).

Ganos Fault where it enters the Marmara Sea is covered by alluvium but a dent on the coast line is taken as the point, where the fault enters the Sea (Altınok et al., 2003; Altunel et al., 2004). Note the very different morphology and landscape north and south of the Ganos Fault.

The village of Gaziköy is located immediately south of the Ganos Fault. In the late 19th century Gaziköy (Ganos) was a large and rich Greek village; it was completely destroyed during

the 1912 Ganos earthquake. After the 1912 earthquake and the officially agreed exchange of Greek and Turkish populations in 1923, the region never recovered its former state.

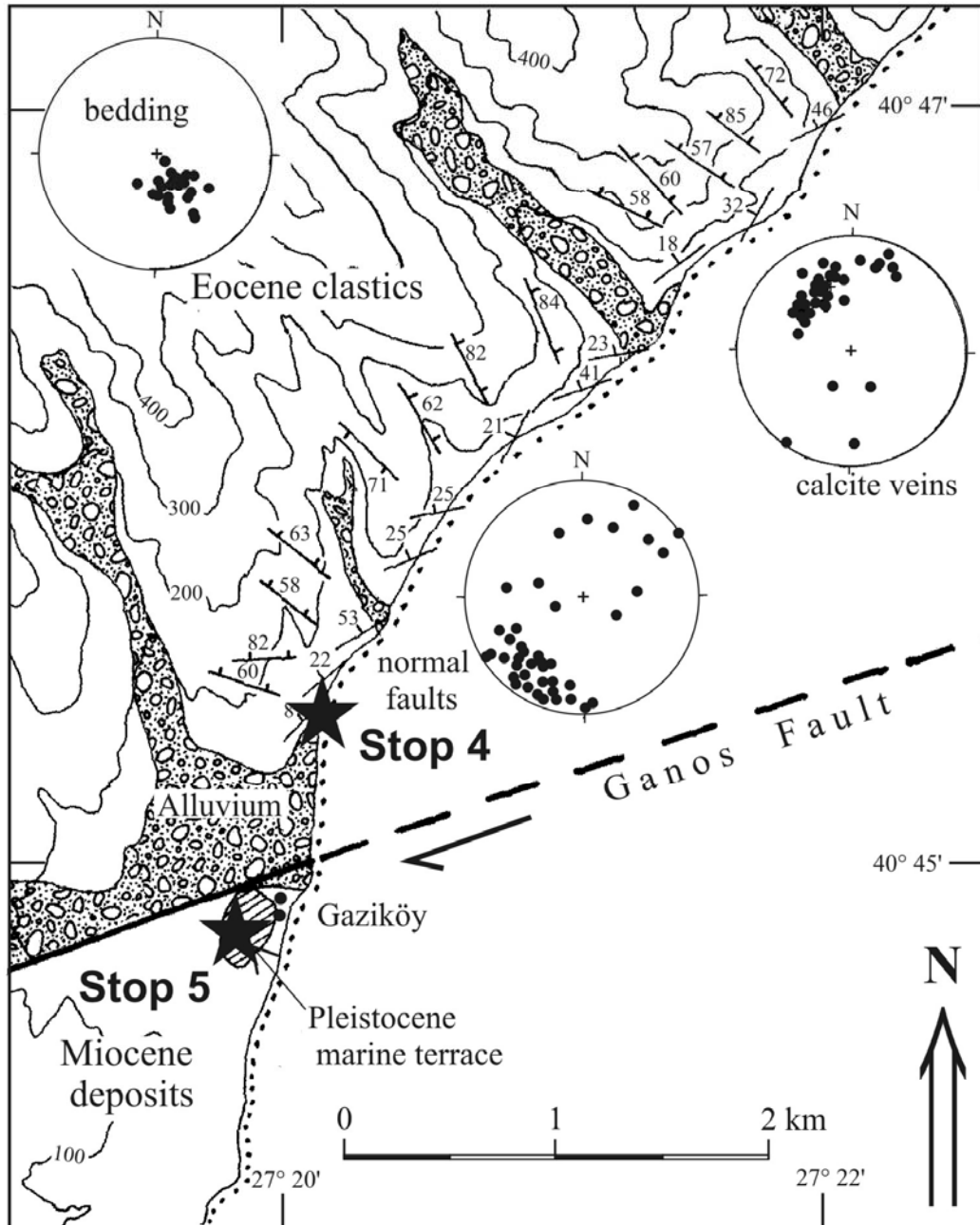


Fig. 18. Structural map of the coastal section northeast of Gaziköy, where the Ganos Fault enters the Marmara Sea. The stereograms show poles to the bedding, to the mesoscopic fault planes and to the extensional calcite veins. Topographic contours are at every 100 m. For illustrative purposes representative mesoscopic faults on the coastal exposures are projected a few hundred meters inland (from Okay et al., 1999).

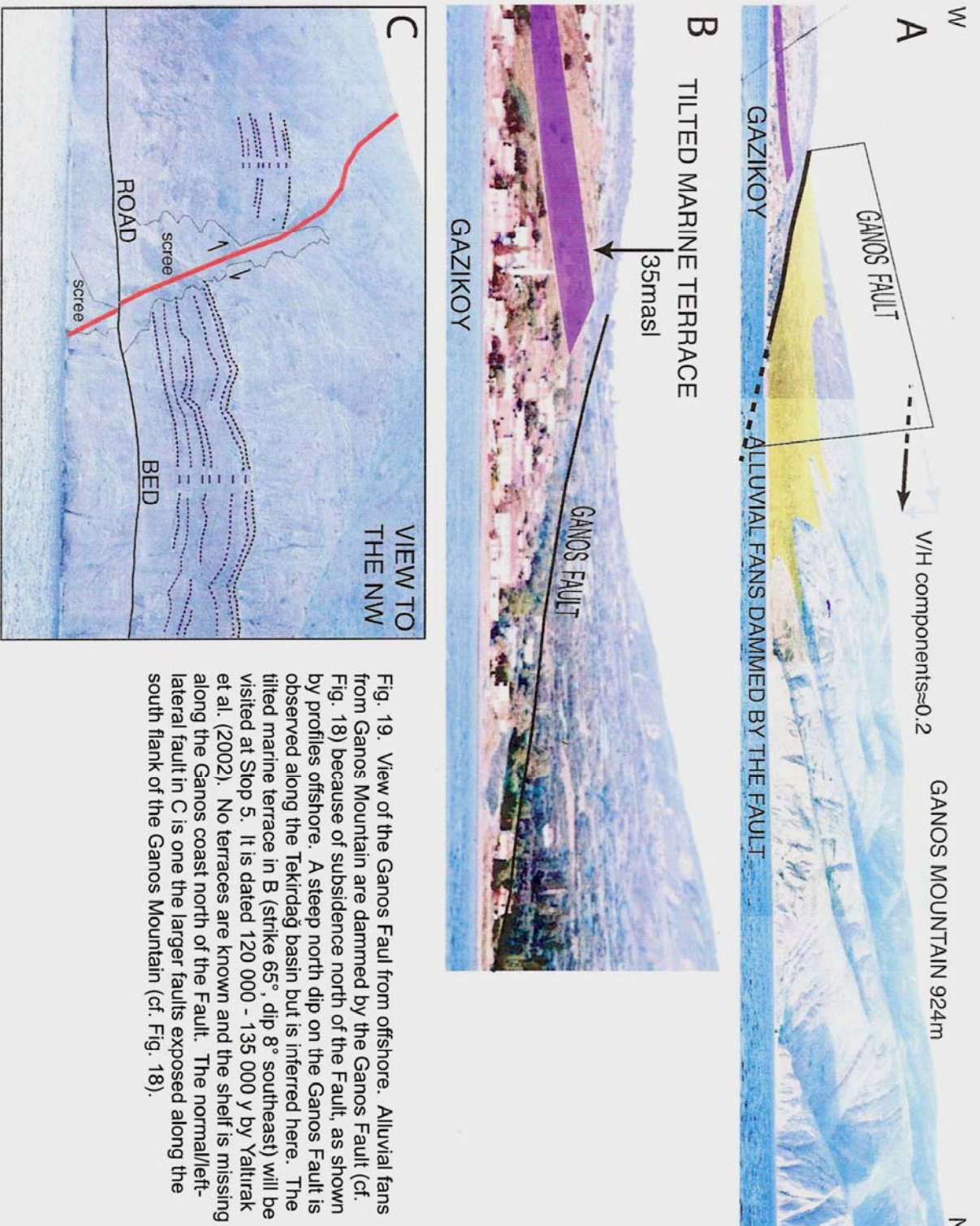


Fig. 19. View of the Ganos Fault from offshore. Alluvial fans from Ganos Mountain are dammed by the Ganos Fault (cf. Fig. 18) because of subsidence north of the Fault, as shown by profiles offshore. A steep north dip on the Ganos Fault is observed along the Tekirdag basin but is inferred here. The tilted marine terrace in B (strike 65° , dip 8° southeast) will be visited at Stop 5. It is dated 120 000 - 135 000 y by Yaltrak et al. (2002). No terraces are known and the shelf is missing along the Ganos coast north of the Fault. The normal/left-lateral fault in C is one the larger faults exposed along the south flank of the Ganos Mountain (cf. Fig. 18).

Stop 5. The Gaziköy marine terrace deposits

Location. Gaziköy (formerly Ganos) village (Figs. 18 and 19a,b)

Interest: Uplifted Pleistocene marine deposits

Description: The hill behind (west) the village of Gaziköy is made up of Late Pleistocene marine deposits. The Gaziköy terrace deposit is located a few hundred meters south of the Ganos Fault (Fig. 18). It is composed of a 36-m-thick sedimentary package, which is tilted $\sim 17^\circ$ to the southwest, resting with angular unconformity over the Middle-Upper Miocene sandstones (Yaltrak et al., 2002). The base of the succession lies at 21,5 m and 14,0 m elevations in the north and south, respectively.

Ten sedimentary packages are differentiated in the Gaziköy terrace deposits (Fig. 20). The basal unit (G0) is unconsolidated pebble conglomerate containing several 3-4-m-wide, and 1-m-deep channels. The conglomerate includes rare specimens of the terrestrial gastropod *Helix* spp. Unit G1 is an upward fining boulder to pebble conglomerate with a sandy matrix, and comprises abundant marine gastropods and bivalves, mainly *Ostrea edulis* colonies. The next unit, G2 consists of fine-grained laminated and weakly carbonate cemented sandstone with abundant sponge spicules and marine macro fossils, including intact specimens *Ostrea edulis*, *Cerithium* spp., *Pecten* spp. and *Acra noae*. An *Arca noae* shell from this level produced a U/Th age of 133.5 ka (Yaltrak et al., 2002). Unit G2 is overlain by the massive, fine-grained sandstones of Unit G3 with carbonate concretions and sponge spicules. Units G4-G6 consists of medium to well cemented sandstones, 10-m-thick, with many in situ *Ostrea* and *Balanus* colonies, separated by a thin unconsolidated fine-grained fossiliferous sandstone (G5). Unit G7 rests on an unconformity, and is a thin pebble conglomerate with abundant marine bivalves, succeeded by a pebbly sandstone with abundant marine bivalves and gastropods (G8) and a bivalve bearing pebble conglomerate (G9). A shell of *Ostrea edulis* from unit G8 produced a U/Th age of 123.1 ka (Yaltrak et al., 2002). Non-fossiliferous, poorly sorted coarse conglomerates (G10) lies unconformably over the marine deposits of G9.

After Gaziköy we follow the coastal road towards Hoşköy (Hora) and Mürefte. The dark and forbidding landscape of the Ganos Mountain is replaced by the soft hills made up of poorly cemented Miocene sandstones, home to extensive vineyards. The region south of the Ganos Fault is one of the largest wine producing areas in Turkey, and the town of Mürefte is the home to one of the two largest vine producers (Doluca). From Mürefte we take the road towards the village of Tepeköy passing through the Miocene sandstones. The first oil in Turkey was produced from these Miocene sandstones just before the First World War. Above Tepeköy we see the hill of Doluca made up of Upper Eocene limestones, which are overlain unconformably

by the Miocene sandstones. The Eocene siliciclastic-carbonate sequence south of the Ganos Fault is exposed in the cores of faulted anticlines. We will drive through the village of Çengelli and take a rough road to reach the top of Doluca Hill at a height of 690 m.

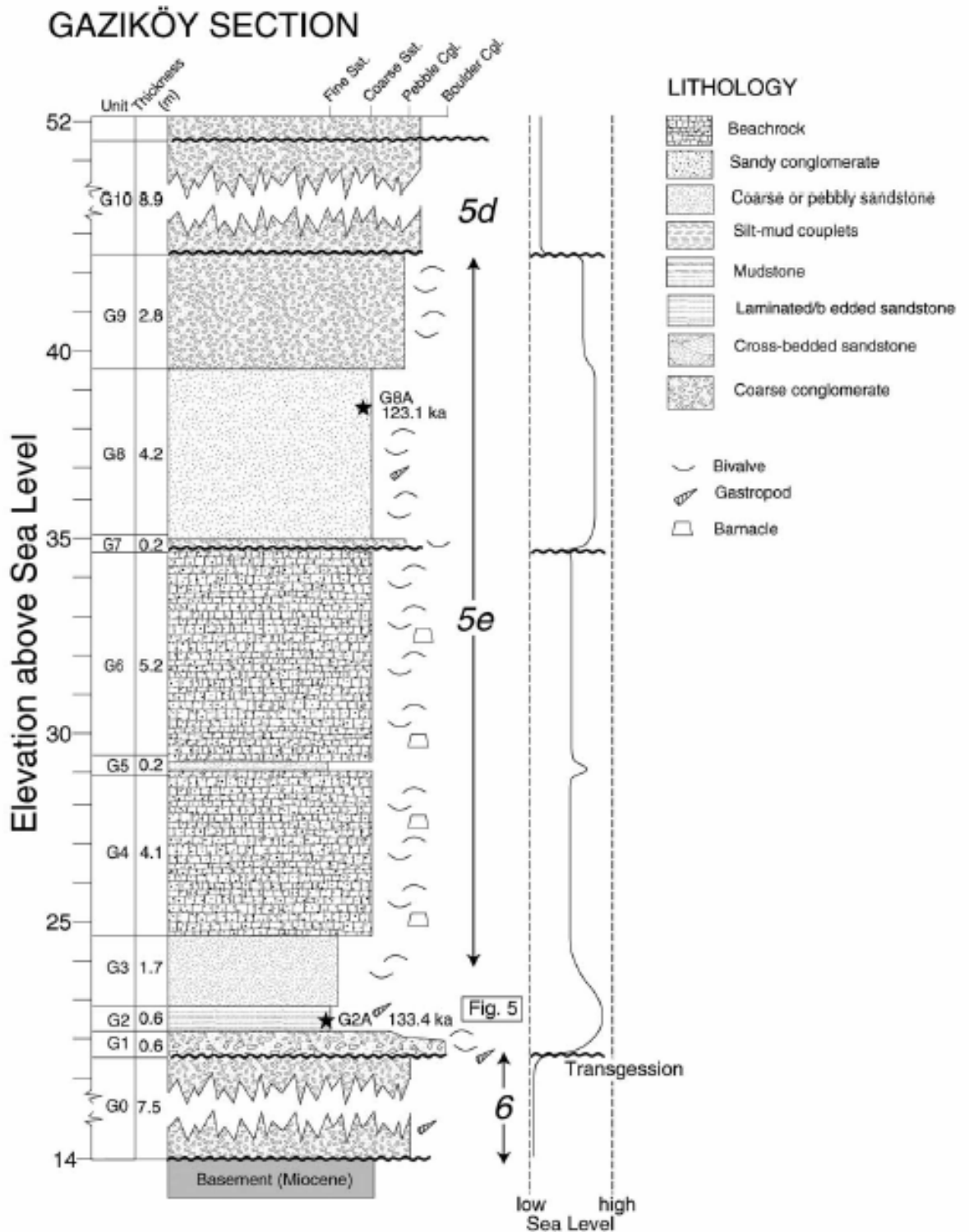


Fig. 20. Measured section of the Pleistocene marine terrace deposits at Gaziköy. See Fig. 17 for location. G0-G10 are lithostratigraphic units discussed in the text. Filled stars with G designations represent locations of shells dated by U/Th technique. Bold numbers 6, 5e and 5d with vertical arrows are global oxygen isotopic stages (from Yaltrak et al., 2002).

Route B

If the road to Gaziköy is closed, we have to drive back 6.5 km from Stop 3 to the junction north of the village of Meryem. From the junction, we take the road to the left (west) towards the Işıklar village. The meter is set to zero at the junction. The road we have taken follows the northern margin of the Ganos Mountain parallel to the monoclinial hinge. We pass through the villages of Işıklar and Oruçbeyli at 5.4 km and 9.2 km, respectively. After Işıklar village there is a good view of the sharp change in topography towards the Ganos Mountain. The sharp change in the slope angles coincides within ± 50 m with the monoclinial hinge suggesting that the landscape is also being deformed.

At 13.4 km we come across a main road junction and take the road to the left marked Şarköy, Gaziköy and Hoşköy. Driving on we pass through the villages of Araphacı (21.2 km) and Tatarlı (24.4 km) and come across a road junction at 27.8 km. Here, we will leave the main road and take the side road marked Ormanlı, Güzelköy, Hoşköy and Gaziköy, which will take us across the Ganos Mountain. The road passes through the village of Ormanlı and then climbs up towards the hills. On the way up there are several good exposures of steeply dipping, recumbently folded sandstones and shales of the Keşan Formation. The top of the mountain marked by a cross-roads is reached at 39.5 km and then we start descending towards the Marmara Sea.

Stop 6 - View of the Ganos Fault from the south

Location: 43.5 km; on the road between Ormanlı and Güzelköy villages, on the southern flank of the Ganos Mountain (Fig. 6) (UTM 05 23 694 - 45 11 588; 40°45.252' - 27°16.840')

Interest: Panoramic view of the Ganos Fault zone

Description: From this vantage point, there is good view to the Ganos Fault, which follows an alluvial valley. Miocene sandstones make up the smooth landscape south of the Fault, whereas the Eocene turbidites make up the forbidding mountain landscape. The small flat topped hill at Gaziköy on the Marmara coast consists of the Pleistocene marine terrace deposits (location of Stop 5). The village of Güzelköy can be seen just below us. The Ganos Fault passes immediately south of the village.

Stop 7 - 9th August 1912 Ganos earthquake surface break

Location: 47.4 km; immediately south of the village of Güzelköy (Fig. 6) (G18-d2) (UTM 05 24 798 - 45 10 104; 40°44.448' - 27°17.621'). Take the small footpath to the right (east) just after the village. Opposite the footpath there is a space for parking the cars.

Interest: surface break of the 9th August 1912 Ganos earthquake

Description: This is one locality described and illustrated in Altunel et al. (2004) as the surface break of the 7.8.1912 Ganos earthquake. The pavement is displaced in a dextral sense.

Along with the geology, the landscape also changes south of Güzelköy. We are now in the southern block of the Ganos Fault characterized by vineyards and olive orchards growing on the poorly cemented Miocene sandstones. We cross the Miocene sandstones and join the main coastal road between Hoşköy and Gaziköy at 51.2 km. At the junction we will turn left (west) and visit Stops 4 and 5. After visiting these Stops, we will drive back to the junction at 51.2 km, and drive towards Hoşköy. There are good outcrops of variegated sandstones of the Miocene Gazhanedere Formation between Hoşköy and Mürefte. At 59.5 km we are in Mürefte. From Mürefte we take the village road to Tepeköy. To reach Tepeköy we take the road north from the centre of Mürefte next to the İş Bank booth, at the end of this road we turn left and follow a tarmac road, which climbs up north passing through the villages of Yukarı Kalamış, Tepeköy and Çengerli (at 84.9 km) (Fig. 21). At 86.6 km we come to a road junction marked Yaya and Yörgüç and turn right towards the villages of Yaya and Yörgüç. At 88.9 km we take a dirt road to the right to drive up the hill of Doluca.

Stop 8 - Panoramic view of the Ganos Fault from the Doluca Hill

Location: 90.8 km, Northwest of the village of Tepeköy (Figs. 6 and 21) (G18-d2) (UTM 05 15 096 - 45 04 345; 40°41.349' - 27°10.719'). Take the dirt road, which branches off from the road between Şarköy and the villages of Yaya and Yörgüç). The road junction is at (UTM 05 14 112 - 45 04 962; 40°41.684' - 27°10.021')

Interest: Panoramic view of the Ganos Fault between the Marmara and Aegean seas.

Description: The Doluca Hill, made up of Middle-Upper Eocene limestones, forms the highest peak south of the Ganos Fault. On a clear day, there is a magnificent view to the Ganos Fault Zone from top of the Doluca Hill. In the afternoon looking eastward, the villages of Yörgüç, Yaya and Mursallı, and Güzelköy in the distance can be seen aligned along the Ganos Fault (Figs. 6 and 21). In the early morning looking westward the Ganos Fault can be followed to the Bay of Saros. The hills of Cinbasarkale and Helva mark the edge of the southern block in the west.

Closer to the Doluca Hill, notice the broad forested hill to the northeast (55°) with a wide meandering forest road on top. It is made up of Eocene siliciclastic rocks, which lie beneath the Middle-Upper Eocene limestones that make up the hill (Fig. 21). To the east (65°) there are overlain by the variegated Miocene sandstones of the Gazhanedere Formation.

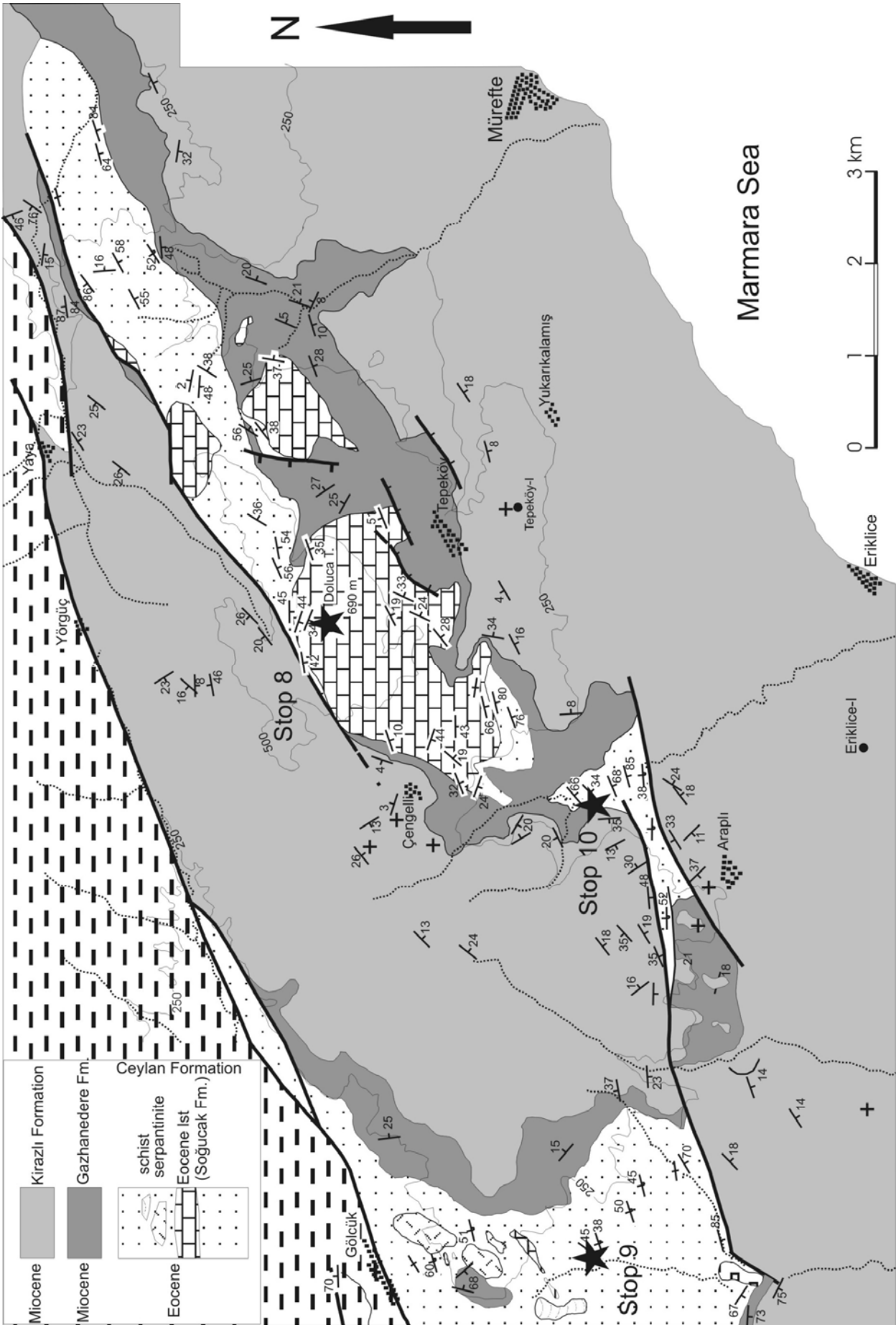


Fig. 21. Geological map of the region of Doluca hill south of Ganos Fault (after Okay unpublished data).

Apatite fission track dating have shown that these Eocene sandstones, of similar age to those

north of the Ganos Fault, were near the surface by the end of Oligocene, while those north of the Fault were at least at 4-5 km depth.

From the Doluca hill we drive back, taking the road towards Şarköy at the Yaya-Yörgüç-Çengelli junction, and join the main İstanbul-Şarköy highway at 100.6 km. On the road between Gölcük and Şarköy the olistostromal Upper Eocene sequence crops out beneath the Miocene cover. There are beautifully exposed serpentinite breccias in a sedimentary carbonate matrix on the hill side overlooking the Ganos Fault near Gölcük (at 40°40.623' - 27°05.325') but it is difficult to stop or park here. Siliciclastic turbidites with grain and debris flows also crop out towards Şarköy.

Stop 9 - Eocene turbidites and debris flows south of the Ganos Fault

Location: North of Şarköy, between Şarköy and the village of Gölcük (Fig. 21) (G18-d1)

Interest: Eocene siliciclastic turbidites south of the Ganos Fault

Description: Sandstones and shales form a folded sequence along this road cut. There is also a conglomerate bed of with Middle-Upper Eocene limestone clasts - a grain flow, which gives the age of the sequence. A sample from this locality gave a late Oligocene (24.7 Ma) apatite fission track age (Zattin et al., 2005).

Optional Stop 10- Angular unconformity between the Eocene and Miocene sequences

Location: Northeast of Şarköy, northeast of the village of Araplı (İğdebağları) along the Çengelli Stream (Fig. 21 and 22) (G18-d2). To reach this outcrop take the dirt road opposite the mosque of Araplı, north-northeast of the minaret. The outcrop is at UTM 05 13 442 - 45 01 146.

Interest: Pre-Miocene deformation possibly linked to the Ganos Fault

Description: Along the Çengelli stream the steeply south dipping Eocene beds are overlain unconformably by the subhorizontal Miocene sandstones (Fig. 21), indicating a phase of late Oligocene deformation, possibly associated with the Ganos Fault.

Although an angular unconformity between the Eocene-Oligocene and Miocene sequences south of the Ganos Fault is obvious both on a map (Fig. 21) and on an outcrop scale (Fig. 22), Armijo et al. (1999) regarded the Eocene-Miocene sequence south of the Ganos Fault as continuous, and instead claimed the existence of a latest Miocene-Pliocene unconformity, for which there is no evidence (see Yaltrak et al. 2000). This latest Miocene-Pliocene "unconformity" was claimed to represent the arrival of the North Anatolian Fault in the Marmara region.



Fig. 22. The unconformity between the steeply dipping Eocene limestones and the overlying subhorizontal Miocene sandstones on the Çengelli stream, west of the Araplı village.

Optional Stop 11 - Blueschists and serpentinite

Location: South of Yeniköy (Figs. 2 and 23) (G18-d1). To reach the blueschists take the road from Şarköy towards Gelibolu. About 1.5 km before the village of Yeniköy, take the forest dirt road to the left (south). The road cuts through the olistostromal Eocene turbidites for about 2.5 km, then a road branches off to the forest hut on top of the Helva Tepe. The blueschists are exposed near the top of the hill.

Interest: Blueschists and serpentinites, probably large blocks in the Eocene flysch.

Description: There are many similarities between the geologies of Turkey and California, and one is the presence of extensive blueschist terranes. South of Yeniköy a ridge made up of serpentinite, diabase, blueschist and an unconformably cover of Upper Eocene limestone forms a positive flower structure and is thrust over the Miocene sequences (Fig. 23). The blueschists are mainly metabasites with sodic amphibole + lawsonite assemblages; there are also some marble and metachert horizons. Preliminary isotopic dating indicate a late Cretaceous metamorphic age (Gültekin Topuz pers. comm.). During the Eocene an oceanic accretionary complex apparently formed the southern margin of the Thrace basin; this is compatible with its fore-arc origin (Görür and Okay, 1996).

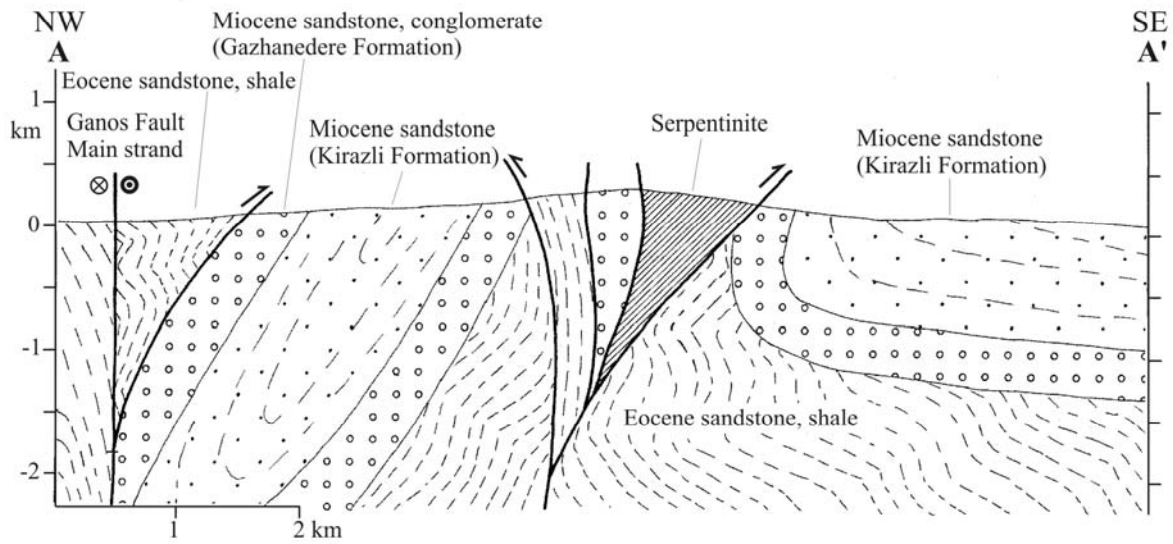
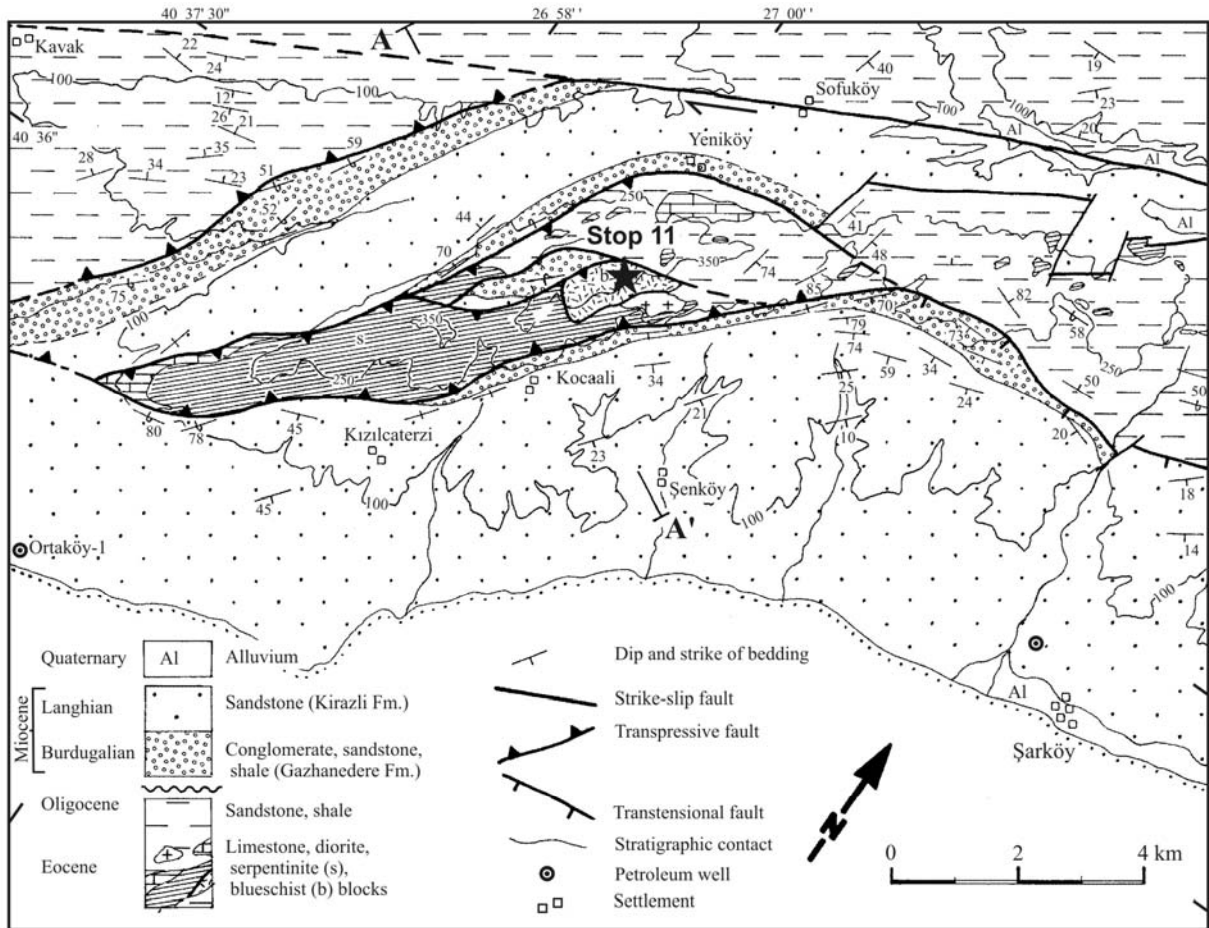


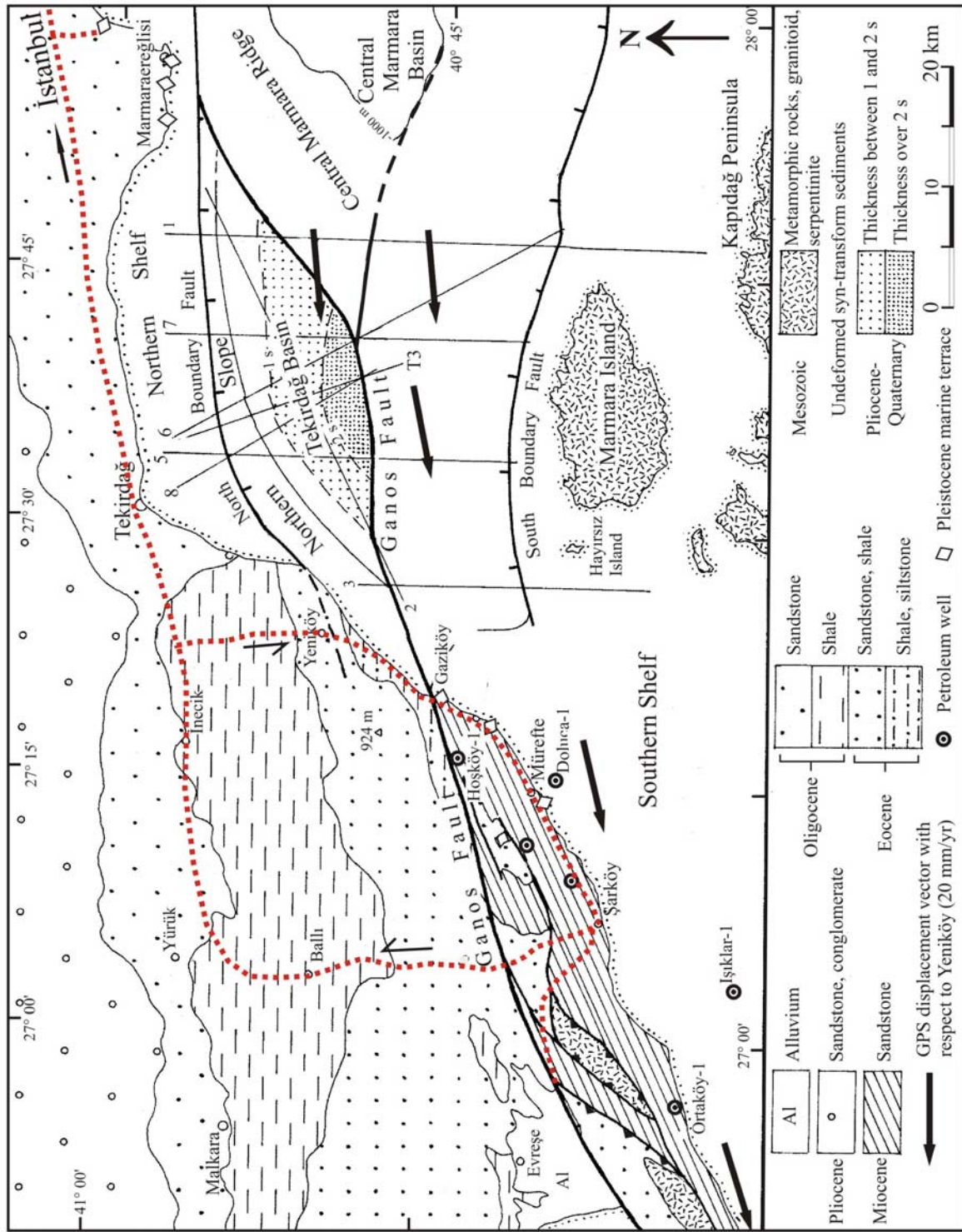
Fig. 23. Geological map and cross-section of the Ganos Fault Zone north of Şarköy (after Okay et al., 1999). For location see Fig. 2.

CITED REFERENCES

- Altınok, Y., Alpar, B., Yalıtırak, C., 2003, Şarköy-Mürefte 1912 Earthquake's Tsunami, extension of the associated faulting in the Marmara Sea, Turkey. *J. Seismology*, 7, 329-346.
- Altunel, E., Meghraoui, M., Akyüz, S., Dikbaş, A., 2004, Characteristics of the 1912 co-seismic rupture along the North Anatolian Fault Zone (Turkey): implications for the expected Marmara earthquake. *Terra Nova*, 16, 198-204.
- Ambraseys, N.N., Finkel, C.F., 1987. The Saros-Marmara earthquake of 9 August 1912. *Earthquake Eng. Struc. Dynamics* 15, 189-211.
- Armijo, R., Meyer, B., Hubert, A., Barka, A., 1999. Westward propagation of the North Anatolian fault into the northern Aegean: Timing and kinematics. *Geology* 27, 267-270.
- Armijo, R., Meyer, B., Navarro, S. King, G., Barka, A., 2002. Asymmetric slip partitioning in the Sea of Marmara pull-apart: a clue to propagation processes of the North Anatolian Fault? *Terra Nova* 14, 80-86.
- Barka, A.A., 1992, The North Anatolian fault Zone. *Ann. Tectonicae*, 6, 164-195.
- Demirbağ, E., Rangin, C., Le Pichon X., Şengör, A.M.C., 2003. Investigation of the tectonics of the Main Marmara Fault by means of deep-towed seismic data. *Tectonophysics* 361, 1-19.
- Donath, F.A., Parker, R.B., 1964. Folds and Folding. *Geol. Soc. Am. Bull.* 75, 45-62.
- Görür, N., Okay, A.I., 1996. A fore-arc origin for the Thrace Basin, NW Turkey. *Geol. Rundschau* 85, 662-668.
- Görür, N., Çağatay, M.N., Sakıncı, M., Sümengen, M., Şentürk, K., Yalıtırak, C., Tchapylyga, A., 1997, Origin of the Sea of Marmara as deduced from Neogene to Quaternary paleobiogeographic evolution of its frame. *Int. Geol. Rev.*, 39, 342-352.
- Hancock, P.L., Erkal, T., 1990. Enigmatic normal faults within the European sector of the North Anatolian transform fault zone, *Ann. Tecton.* 4, 171-181.
- Harland, W.B., 1971. Tectonic transpression in Caledonian Spitsbergen. *Geol. Mag.* 108, 27-42.
- Hubert-Ferrari A., Armijo, R., King, G., Meyer, B., Barka, A., 2002. Morphology, displacement, and slip rates along the North Anatolian Fault, Turkey. *J. Geophys. Res.*, 107 (B10): art. no. 2235.
- Jamison, W.R., 1991. Kinematics of compressional fold development in convergent wrench terranes. *Tectonophysics* 190, 209-232.
- Kopp, K.O., Pavoni N., Schindler C., 1969. *Geologie Thrakiens IV: Das Ergene Becken.* Beihefte Geol Jahrbuch 76, 1-136.
- Lebküchner, R.F., 1974. Beitrag zur Kenntnis des Geologie des Oligozäns von MittelThrakien (Türkei). *Bull. Mineral Res. Expl. Ins. Turkey* 83, 1-30.
- Le Pichon, X., Şengör, A.M.C. Demirbağ, E., Rangin, C., İmren, C. Armijo, R., Görür, N., Çağatay, N., Mercier de Lepinay, B., Meyer, B., Saatçiler, R., Tok, B., 2001. The active Main Marmara Fault. *Earth Planet. Sc. Lett.* 192, 595-616.
- McClusky S, Balassanian S, Barka A, et al., 2000, Global Positioning System constraints on plate kinematics and dynamics in the eastern Mediterranean and Caucasus. *J. Geophys. Res.*, 105, 5695-5719.
- Meade, B.J., Hager, B.H., McClusky, S.C., Reilinger, R.E., Ergintav, S., Onur, L., Barka, A. Özener, H., 2002, Estimates of seismic potential in the Marmara Sea region from block models of secular deformation constrained by Global Positioning System measurements. *Bull. Seismol. Soc. Am.* 92, 208-215.
- Okay, A.I., Demirbağ, E., Kurt, H., Okay, N., Kuşçu, İ., 1999. An active, deep marine strike-slip basin along the North Anatolian fault in Turkey. *Tectonics* 18, 129-148.
- Okay, A. I., Kaşlılar-Özcan, A., İmren, C., Boztepe-Güney, A., Demirbağ, E., Kuşçu, İ., 2000. Active faults and evolving strike slip basins in the Marmara Sea, northwest Turkey: a multi-channel seismic reflection study. *Tectonophysics* 321, 189-218.
- Okay, A.I., Tüysüz, O. & Kaya, Ş., 2004, From transpression to transtension: Changes in morphology and structure around a bend on the North Anatolian Fault in the Marmara region. *Tectonophysics*, 391, 259-282.
- Okay, N., Okay, A.I., 2002, Tectonically induced Quaternary drainage diversion in northeastern Aegean. *J. Geol. Soc. Lond.* 159, 393-400.
- Polonia, A., Cormier, M.H., Çağatay, N., Bortoluzzi, G., Bonatti, E., Gasperini, L., Seeber, L., Görür, N., McHugh, C., Ryan, W.B., Emre, Ö., Okay, N., Ligi, M., Tok, B., Blasi, A., Buseti, M., Eriş, K., Fabretti, P., Fielding, E.J., İmren, C., Kurt, H., Magagnoli, A., Marozzi, G., Özer, N., Penitenti, D., Serpi, G., ve Sarıkavak, K., Exploring submarine earthquake geology in the Marmara Sea, *EOS Transactions* 83 (21), 229 and 235-236.
- Rangin, C., Demirbağ, E., İmren, C., Crusson, A., Normand, A., Le Drezen, E., Le Bot, A., 2001, *Marine Atlas of the Sea of Marmara (Turkey)*, Ifremer.
- Şaroğlu, F., Emre, Ö., Kuşçu, İ., 1992. Active fault map of Turkey. *Maden Tetkik ve Arama Genel Müdürlüğü*, Ankara, Turkey, 2 sheets, scale 1: 2, 000, 000.
- Seeber, L., Emre, O., Cormier, M., Sorlien, C., McHugh, C., Polonia, A., 2004. Uplift and subsidence from oblique slip: the Ganos-Marmara bend of the North Anatolian Transform, western Turkey. *Tectonophysics*, 391, 239-258.
- Şengör, A.M.C., 1979. The North Anatolian transform fault: Its age, offset and tectonic significance. *J. Geol. Soc. London* 136, 269-282.
- Şengör, A.M.C., Tüysüz, O., İmren, C., Sakıncı, M., Eyidoğan, H., Görür, N., Le Pichon, X., Rangin, C., 2005, The North Anatolian Fault: a new look. *Annual Reviews of Earth and Planetary Sciences*, 33, 37-112.

- Şentürk, K., Sümengen, M., Terlemez, İ., Karaköse, C., 1998. Bandırma D-4 sheet and explanatory text, 1:100 000 scale geological map series, Maden Tetkik ve Arama Genel Müdürlüğü, Ankara 10 p.
- SHOD - Seyir, Hidrografi ve Oşinografi Dairesi Başkanlığı, 1983, Bathymetric chart of the Marmara Sea between Büyükçekmece and Hoşkøy, scale 1:100 000 (Map No. 291).
- SHOD - Seyir, Hidrografi ve Oşinografi Dairesi Başkanlığı, 1988, Bathymetric chart of the Marmara Sea between Hoşkøy and Gelibolu, scale 1:75 000 (Map No. 295).
- Sylvester, A.G., 1988. Strike-slip faults. *Geol. Soc. Am. Bull.* 100, 1666-1703.
- Turgut, S., Türkaslan, M., Perinçek, D., 1991. Evolution of the Thrace sedimentary basin and its hydrocarbon prospectivity. In: Spencer, A.M. (Ed.), *Generation, Accumulation, and Production of Europe's Hydrocarbons. Spec. Publ. Euro. Ass. Petrol. Geoscient.* 1, 415-437.
- Tüysüz, O., Barka, A., Yiğitbaş, E. 1998. Geology of the Saros Graben: its implications on the evolution of the North Anatolian Fault in the Ganos-Saros region, NW Turkey. *Tectonophysics* 293, 105-126.
- Yaltrak, C., 1996, Tectonic history of the Ganos Fault System (in Turkish). *Turk. Assoc. Petr. Geol. Bull.*, 8, 137-156.
- Yaltrak, C., Alpar, B., 2002. Kinematics and evolution of the northern branch of the North Anatolian Fault (Ganos Fault) between the Sea of Marmara and the Gulf of Saros. *Mar. Geol.* 190, 352-366.
- Yaltrak, C., Sakınç, M., Oktay, F.Y., 2000, Westward propagation of the North Anatolian fault into the northern Aegean: Timing and kinematics, *Comment. Geology*, 28, 187-188.
- Yaltrak C., Sakınç, M., Aksu, A.E., Hiscott, R.N., Galeb, B., Ulgen, U.B., 2002, Late Pleistocene uplift history along the southwestern Marmara Sea determined from raised coastal deposits and global sea-level variations, *Marine Geol.*, 190, 283-305.
- Zattin, M., Okay, A.I. & Cavazza, W., 2005. Fission-track evidence for late Oligocene and mid-Miocene activity along the North Anatolian Fault in south-western Thrace. *Terra Nova*, 17, 95-101.

NOTES



The red dotted line shows the itinerary of the Ganos field trip on the 18th August 2006.